

**ISTANBUL TECHNICAL UNIVERSITY ★ GRADUATE SCHOOL OF SCIENCE**  
**ENGINEERING AND TECHNOLOGY**

**NUMERICAL AND EXPERIMENTAL INVESTIGATION OF BIOINSPIRED  
SOFT ROBOTIC ACTUATOR THAT CREATES VACUUM**



**M.Sc. THESIS**

**Umut Serdar ÇİVİCİ**

**Department of Mechanical Engineering**

**Mechanical Design Program**

**JULY 2020**



**ISTANBUL TECHNICAL UNIVERSITY ★ GRADUATE SCHOOL OF SCIENCE**  
**ENGINEERING AND TECHNOLOGY**

**NUMERICAL AND EXPERIMENTAL INVESTIGATION OF BIOINSPIRED  
SOFT ROBOTIC ACTUATOR THAT CREATES VACUUM**



**M.Sc. THESIS**

**Umut Serdar ÇİVİCİ**  
**(503171222)**

**Department of Mechanical Engineering**

**Mechanical Design Program**

**Thesis Advisor: Asst. Prof. Zeynep PARLAR**

**JULY 2020**



**İSTANBUL TEKNİK ÜNİVERSİTESİ ★ FEN BİLİMLERİ ENSTİTÜSÜ**

**TASARIMINDA DOĞADAN ESİNLENİLMİŞ VE VAKUM KUVVETİ  
YARATABİLEN YUMUŞAK ROBOTİK AKTÜATÖRÜN NÜMERİK VE  
DENEYSEL İNCELENMESİ**

**YÜKSEK LİSANS TEZİ**

**Umut Serdar ÇİVİCİ  
(503171222)**

**Makina Mühendisliği Anabilim Dalı**

**Konstrüksiyon Programı**

**Tez Danışmanı: Dr. Öğr. Üyesi Zeynep PARLAR**

**TEMMUZ 2020**



Umut Serdar IVICI, a M.Sc. student of ITU Graduate School of Science Engineering and Technology student ID 503171222, successfully defended the thesis/dissertation entitled “NUMERICAL AND EXPERIMENTAL INVESTIGATION OF BIOINSPIRED SOFT ROBOTIC ACTUATOR THAT CREATES VACUUM”, which he prepared after fulfilling the requirements specified in the associated legislations, before the jury whose signatures are below.

**Thesis Advisor :** **Asst. Prof. Zeynep PARLAR**  
İstanbul Technical University

**Jury Members:** **Assoc. Prof. Orhan AKIR**  
Yıldız Technical University

**Asst. Prof. Merve Acer KALAFAT**  
İstanbul Technical University

**Date of Submission : 15 June 2020**  
**Date of Defense : 16 July 2020**



*To Everyone Who Loves Science,*





## **FOREWORD**

Firstly, I would like to express my gratefulness to my supervisor, Asst. Prof. Dr. Zeynep PARLAR. You have been a great mentor and a teacher for me. I am grateful for your full support and broaden my horizon. Your recommendations for my research as well as on my career have been treasure.

Special thanks to my partner Ceyda DÖNMEZ with the help of everything in this way of my life. Your speeches at every difficult moments have been a great support for me. Besides, in manufacturing of the soft robot, your ideas made great value in the processes.

I would like to thank Ferit YILDIZ and Cüneyt BAYRAM for the helps, ideas, and components for experimental works.

Moreover, I would like to thank my family for supporting me all the time and especially in this time of my life.

At the end, I hope this study will add value to the soft robotic research.

July 2020

Umut Serdar ÇİVİCİ  
(Mechanical Engineer)



## TABLE OF CONTENTS

	<u>Page</u>
<b>FOREWORD</b> .....	<b>ix</b>
<b>TABLE OF CONTENTS</b> .....	<b>xi</b>
<b>ABBREVIATIONS</b> .....	<b>xiii</b>
<b>LIST OF TABLES</b> .....	<b>xv</b>
<b>LIST OF FIGURES</b> .....	<b>xvii</b>
<b>SUMMARY</b> .....	<b>xix</b>
<b>ÖZET</b> .....	<b>xxi</b>
<b>1. INTRODUCTION</b> .....	<b>1</b>
1.1 Purpose and Workflow of Thesis .....	3
1.2 Literature Review .....	4
<b>2. ADHESION AND SUCTION FORCE PHENOMENA</b> .....	<b>9</b>
2.1 Adhesion Mechanisms .....	9
2.2 Suction Mechanism and Suction Force.....	10
2.2.1 Suction cups .....	10
2.2.2 Bio Inspirational design .....	12
2.2.3 Physic and calculation of suction mechanism .....	12
<b>3. DESIGN OF SOFT ROBOT</b> .....	<b>15</b>
3.1 Soft Robot Segmentation .....	15
3.2 Design Parameters .....	17
3.2.1 Parameters effect on vacuum performance .....	19
3.2.2 Parameters used in calculations .....	19
<b>4. EXPERIMENTAL STUDY</b> .....	<b>21</b>
4.1 Manufacturing Methods .....	22
4.2 Experimental Set Ups .....	27
4.3 Control and Testing.....	30
<b>5. NUMERICAL STUDY</b> .....	<b>33</b>
5.1 Parametric Finite Element Analysis Study .....	33
5.1.1 Finite element analysis matrix .....	34
5.2 Finite Element Analysis Model Set Up.....	35
5.2.1 Unit system, ABAQUS .....	36
5.2.2 Material models .....	37
5.2.3 Contact models.....	40
5.2.4 Boundary conditions .....	41
5.2.5 Fluid cavity module, ABAQUS .....	43
5.2.6 Mesh model.....	44
<b>6. RESULTS AND DISCUSSION</b> .....	<b>47</b>
6.1 Experimental Results .....	48
6.2 Finite Elementa Analysis Model Validation .....	49
6.3 Finite Element Analysis Results .....	49
6.4 Discussion .....	58
<b>7. CONCLUSION</b> .....	<b>61</b>
<b>8. REFERENCES</b> .....	<b>63</b>



## **ABBREVIATIONS**

<b>FEA</b>	: Finite Element Analysis
<b>BSRA</b>	: Bioinspired Soft Robotic Actuator
<b>DOF</b>	: Degree of Freedom
<b>CAD</b>	: Computer Aided Design
<b>SPA</b>	: Soft Pneumatic Actuator
<b>SMA</b>	: Shape Memory Alloy
<b>GA</b>	: Genetic Algorithm
<b>EAP</b>	: Electro Active Polymer
<b>PDMS</b>	: Polydimethylsiloxane
<b>CNC</b>	: Computer Numerical Control
<b>PPAS</b>	: Positive Pressure Actuated Suction-Cup
<b>ACSR</b>	: Amphibious Climbing Soft Robot
<b>SI</b>	: International System of Units
<b>PLA</b>	: Polylactic Acid
<b>ODB</b>	: Output Database
<b>BOM</b>	: Bill of Materials



## LIST OF TABLES

	<u>Page</u>
<b>Table 1. 1</b> : Real Life Example of Soft Robotics.....	5
<b>Table 3. 1</b> : Parameters that affect the vacuum performance.....	19
<b>Table 5. 1</b> : Unit System of FEA in ABAQUS.....	37
<b>Table 5. 2</b> : Material Properties of Ecoflex 00-30. (Yang et al., 2013) .....	39
<b>Table 5. 3</b> : Mooney Rivlin Material Constants, Ecoflex 00-30. (Yang et al., 2013).....	40
<b>Table 5. 4</b> : Material Properties of Paper. (Yang et al., 2013) .....	40
<b>Table 5. 5</b> : Finite Element Mesh Details for Each Design.....	46





## LIST OF FIGURES

	<u>Page</u>
<b>Figure 1. 1</b> : One of the Example of Multi-Gait Soft Robot. (Shepherd et al., 2011)	1
<b>Figure 1. 2</b> : Schematic of the Soft Robot, a) Stationary, b) Inflated with Air.....	2
<b>Figure 1. 3</b> : Workflow of Soft Robotic Research. ....	4
<b>Figure 1. 4</b> : Effect of Material on volume-pressure curve. (A) Extensible material of Ecoflex 30 and inextensible layer of PDMS, (B) extensible material of Elastosil and inextensible layer of paper is used. (Mosadegh et al., 2014) .....	7
<b>Figure 2. 1</b> : Classification of Adhesion Types.....	9
<b>Figure 2. 2</b> : Adhesion Mechanisms. (Bhuse, 2018).....	10
<b>Figure 2. 3</b> : Suction Methods in Suction Cups. ....	11
<b>Figure 2. 4</b> : Working Operations of Suction Cups, (a) Steady phase, (b) Pushing phase, (c) Adhere phase, (d) Detached phase. ....	11
<b>Figure 2. 5</b> : Octopus Sucker, (a) View with grooves and orifice, (b) Cross section of sucker. (Sareh et al., 2017).....	12
<b>Figure 2. 6</b> : Suction Force Calculation. ....	13
<b>Figure 3. 1</b> : Schematic Representation of Soft Robot. ....	15
<b>Figure 3. 2</b> : Cross Sectional View of Five Soft Robot Designs. ....	16
<b>Figure 3. 3</b> : Air Cavity Designs. ....	17
<b>Figure 3. 4</b> : Design Parameters.....	18
<b>Figure 3. 5</b> : Cross Section of the Cavity, a) Before inflation, b) After inflation. ....	18
<b>Figure 4. 1</b> : Process of Experimental Study.....	21
<b>Figure 4. 2</b> : Representative Manufacturing Process of the Soft Robot.....	22
<b>Figure 4. 3</b> : Material Preparation (Ecoflex 0030, Smooth-On Inc.) .....	23
<b>Figure 4. 4</b> : Molding Techniques of the Spiral Design.....	24
<b>Figure 4. 5</b> : Manufactured Molds and Part Details.....	24
<b>Figure 4. 6</b> : Molding of Bottom Part of the Soft Robot.....	25
<b>Figure 4. 7</b> : Demolded Silicone, Bottom Side of the Spiral Design. ....	25
<b>Figure 4. 8</b> : Top Cover Molding. ....	26
<b>Figure 4. 9</b> : Strain Limiting Layer Assembly. ....	26
<b>Figure 4. 10</b> : Final Manufactured Soft Robot.....	27
<b>Figure 4. 11</b> : Bill of Materials (BOM).....	28
<b>Figure 4. 12</b> : Schematic Representation of Experimental Set-Up. ....	29
<b>Figure 4. 13</b> : Detailed Experimental Set-up. ....	30
<b>Figure 4. 14</b> : Compressor Control Arduino Script. ....	31
<b>Figure 4. 15</b> : Connection Diagram of the Electronic Components.....	31
<b>Figure 5. 1</b> : Overview of FEA Model Structure. ....	34
<b>Figure 5. 2</b> : FEA Model Cases for All Designs. ....	34
<b>Figure 5. 3</b> : General FEA Model Set-Up. ....	35
<b>Figure 5. 4</b> : Stress-Strain Curve Comparison, (a) Linear Elastic, (b) Hyperelastic. (Abubakar et al., 2016) .....	38
<b>Figure 5. 5</b> : Ecoflex 00-30 Stress-Strain Curve. (Hsu et al., 2013) .....	39
<b>Figure 5. 6</b> : Schematic of Pure Penalty Contact. ....	41
<b>Figure 5. 7</b> : Contact State of the Soft Robot and Paper Layer.....	41

<b>Figure 5. 8</b> : Fixed Boundary condition of Bottom Surface of the Soft Robot. ....	42
<b>Figure 5. 9</b> : Pressure Boundary Condition of All Designs.....	42
<b>Figure 5. 10</b> : Reference Node and Volume-Pressure Calculation. ....	43
<b>Figure 5. 11</b> : Fluid Cavity Reference Node and Selected Surfaces, a) Selected Surfaces of Fluid Cavity, b) Abaqus Definition of Fluid Cavity. ....	44
<b>Figure 5. 12</b> : 3D 10-Node Tetrahedral Element, 2 <sup>nd</sup> Order.....	45
<b>Figure 5. 13</b> : Mesh Convergence Study Results. ....	46
<b>Figure 6. 1</b> : Experimental Study Results of Reference Model (Spiral Design). ....	48
<b>Figure 6. 2</b> : Validation of the FEA Model with Experimental Results.....	49
<b>Figure 6. 3</b> : Spiral Design FEA Results, a) Vacuum Pressure, b) Suction Force. ...	50
<b>Figure 6. 4</b> : Vacuum Pressure Graph (Spiral Design).....	50
<b>Figure 6. 5</b> : Displacement Result of Spiral Design. ....	51
<b>Figure 6. 6</b> : Semicircular Design FEA Results, a) Vacuum Pressure, b) Suction Force.....	51
<b>Figure 6. 7</b> : Vacuum Pressure Graph (Semicircular Design).....	52
<b>Figure 6. 8</b> : Displacement Result of Semicircular Design. ....	52
<b>Figure 6. 9</b> : Center Spiral Design FEA Results, a) Vacuum Pressure, b) Suction Force.....	53
<b>Figure 6. 10</b> : Vacuum Pressure Graph (Center Spiral Design). ....	53
<b>Figure 6. 11</b> : Displacement Result of Center Spiral Design. ....	53
<b>Figure 6. 12</b> : Circular Design FEA Results, a) Vacuum Pressure, b) Suction Force. .....	54
<b>Figure 6. 13</b> : Vacuum Pressure Graph (Circular Design). ....	54
<b>Figure 6. 14</b> : Displacement Result of Circular Design. ....	55
<b>Figure 6. 15</b> : Vertical Design FEA Results, a) Vacuum Pressure, b) Suction Force. .....	55
<b>Figure 6. 16</b> : Vacuum Pressure Graph (Vertical Design). ....	55
<b>Figure 6. 17</b> : Displacement Result of Vertical Design.....	56
<b>Figure 6. 18</b> : Contact Area and Vacuum Pressure, for Paper Heights: a) 0,1 mm, b) 0,3 mm, c) 0,5 mm. ....	56
<b>Figure 6. 19</b> : Contact Area and Suction Force, for Paper Heights: a) 0,1 mm, b) 0,3 mm, c) 0,5 mm. ....	57
<b>Figure 6. 20</b> : Paper Height and Vacuum Pressure, for Contact Areas: a) 586 mm <sup>2</sup> , b) 950 mm <sup>2</sup> , c) 1290 mm <sup>2</sup> . ....	58
<b>Figure 6. 21</b> : Paper Height and Suction Force, for Contact Areas a) 586 mm <sup>2</sup> , b) 950 mm <sup>2</sup> , c) 1290 mm <sup>2</sup> .....	58

# **NUMERICAL AND EXPERIMENTAL INVESTIGATION OF BIOINSPIRED SOFT ROBOTIC ACTUATOR THAT CREATES VACUUM**

## **SUMMARY**

Robots have become indispensable helpers of humankind after the industrial revolution. Conventional robotic systems are used in various applications from automotive to aerospace industries concerning their stiff and strong structures and doing the tasks on time concurrently. In recent years, due to the desire to create safer robotic systems for people and development in material and control systems, a new field that is called soft robotics has emerged. Its application areas are; artificial muscles used in medicine, soft robotic grippers in manufacturing lines, wearable robotics in human-robot interaction applications such as haptic sensing and feedback, and more importantly soft robots are investigated in to use in space exploration and assembly in Langley's Makerspace Lab at NASA. In the scope of this thesis, the design of bioinspired soft robotic actuator (BSRA) is investigated. Biomimetic and bioinspired design terminologies could be considered the main constituents of soft robotic systems, and these concepts are becoming popular in recent years due to their ability to reflect the nature and overcome the problems that humankind ever have. Moreover, bio-inspired soft robotic designs take inspiration from nature while it mimics the function of biological mechanisms, for instance, octopus' suction effect, gecko's adhesive fibrils, and jellyfish's movement mechanisms. Since abilities of soft robotic systems, bio-inspired soft robotic pneumatic actuators have recently emerged as a new subfield of robotics, their soft and highly deformable material characteristics distinguish their selves from conventional robotic systems.

The goal of this study is to design, computer simulation, fabrication, and test of a soft actuator that creates vacuum and suction force when it is actuated by compressed air. The methodology used in this study is creating a vacuum effect by pressurized air channels inside of soft robot, rather than using conventional suction techniques, which requires a pump that is large in size and heavy machines that sucks the air inside of the air channel. To predict the motion of soft robot and vacuum performance, a comprehensive study of nonlinear finite element analysis (FEA) is conducted by using ABAQUS software with respect to material and geometrical nonlinearities.

The first step in the design procedure is deciding the air channel geometries of a soft robot. In this study, five main air channel geometry is considered which is called the spiral, semicircular, center spiral, circular, and vertical channel. It is observed that the more curvature design of the air channel creates bigger suction force. Investigations are showed that gecko's fibrils and octopus' suction arms have the advanced capabilities on creating adhesive forces on a substrate. Therefore, it is found that octopus' arm geometry is more suitable in order to adapt the design on a soft robotic system. Moreover, octopus' arm is chosen and the outer shape of the soft robot is designed a simplified version of octopus' arm. To have the control of the hyper-elastic material of soft robot, which is possible with adding a more stiff material to a specific

area on the soft robot, an inextensible layer is added to the top face of the vacuum surface. It could be said that paper has tremendously effected the bending performance and chosen as an inextensible (stiffing) layer material.

The second step consists of non-linear FEA, which gives an idea of how soft robot will move and deform when it is actuated and vacuum pressure obtained. To do that numerical study conducted with the help of ABAQUS standard software. In the finite element analysis, material and geometrical nonlinearities are considered. In total 45 FEA, analysis is conducted over five different air channel geometries with respect to paper height and contact area design parameters. In each sub-analysis section for each soft robotic design, nine different FEA analysis is planned with three different levels of correlation to paper height and contact area.

The third step is the manufacturing and testing of the soft robot, which includes material selection, production methods, molding techniques. In order to produce molds, a conventional 3D printer is used with the mold material of PLA. Moreover, the base material of soft robot is chosen, as Ecoflex 0030 (Smooth-On Inc.) due to it is available in the market and resistance to failure when it is actuated with air as well as flexibility. The spiral form of the actuator is chosen as a reference model and it is manufactured to validate FEA model results. The manufactured soft robot is actuated with compressed and vacuum is measured with a pressure sensor.

It is concluded that actuator which has center spiral air channel geometry provided more vacuum and suction force comparing to other proposed air channel geometries. It can be finalized that the center spiral soft robotic actuator can be used in vacuum applications.

# **TASARIMINDA DOĞADAN ESİNLENİLMİŞ VE VAKUM KUVVETİ YARATABİLEN YUMUŞAK ROBOTİK AKTÜATÖRÜN NÜMERİK VE DENEYSEL İNCELENMESİ**

## **ÖZET**

Robotlar sanayi devriminden sonra insanların en büyük yardımcıları olmuşlardır. Gelişen malzeme bilgisi, seri üretime artan talep ve otomasyona geçiş zorunluluğu robotların imalat süreçlerine dâhil olmasını mecbur kılmıştır. Robotlar güçlü, dayanıklı mekanizmaları ve verilen görevi hatasız olarak istenilen zamanda yapmalarından dolayı otomotiv sektöründen havacılık sektörüne kadar çeşitli yerlerde kullanılmışlardır. Robotların kullanım alanlarında çalışan insanlar için yarattığı tehlikeler ve güvenlik sorunları, günümüzde daha güvenli ve insanlar ile etkileşim içinde çalışabilecek olan yumuşak robotların ortaya çıkmasını sağlamıştır. Yumuşak robotların kullanım alanları: tıpta kullanılan yapay kaslar, otomasyon ve imalat süreçlerinde kullanılan tutucular, giyilebilir insan-robot etkileşimli uygulamalar olarak sınıflandırılabilir. Daha da önemlisi bu yenilikçi robot alanı NASA'nın Langley's Makerspace Laboratuvarlarında uzay araştırmaları ve uzayda üretimi konusunda çalışılmaktadır. Bu tez kapsamında, tasarımında doğadan esinlenilmiş yumuşak robotun vakum kabiliyeti nümerik ve deneysel olarak araştırılmıştır. Doğadan esinlenme ve doğayı kopyalama terminolojileri yumuşak robotik sistemlerin temel yapı taşı olarak düşünülebilir. Doğayı yansıtma ve insanlığın sahip olduğu sorunları çözme kabiliyetleri bakımından bu terminolojilerin kullanıldığı uygulamalar günümüzde gittikçe daha da yaygınlaşmaktadır. Doğadan esinlenilmiş yumuşak robot tasarımları ilham kaynağı olarak doğayı almalarının yanı sıra biyolojik mekanizmaların fonksiyonlarını kopyalayarak insan hayatına girmektedir. Bu tasarımlara, ahtapotların vakum kabiliyetlerinden faydalanılarak tasarlanmış vantuzlar, geckonun adeziv fibrillerinden esinlenilerek üretilmiş yapılar ve denizanasının hareket mekanizmasını yansıtan mekanizmalar örnek olarak verilebilir. Yumuşak robotların bu kabiliyetlerinin yanı sıra, malzemelerinin yumuşak, elastik, deforme olmaya elverişli olmaları ve serbestlik derecelerinin fazla olması onları konvansiyonel robotik sistemlerden ayırır.

Bu çalışmanın ana amacı, hava ile tahrik edilebilen ve vakum kuvveti yaratabilecek yumuşak bir robotu tasarlamaktır. Bu tezde yöntem olarak vakum kuvvetini konvansiyonel vakum pompaları ile yapmak yerine, yumuşak robotun kubbe halini almasını sağlayarak vakum kuvveti oluşturmaktır. Yumuşak robotların hem lineer olmayan yapılarından dolayı (gerek malzeme gerekse hareketleri sonucu büyük deformasyona uğramaları), hareketlerinin tahmini ve kontrolünü sağlamak için sonlu elemanlar yöntemi kullanılmaktadır. Bu tezde yumuşak robotların tahrik yöntemlerinden biri olan hava akışının modellenmesi ve akış-katı analizinin sonuçları, sadece katı analizi yapılarak (gaz basıncının duvarlara uygulanması) elde edilen sonuçlar ile örtüştüğü için zaman ve hesaplama olarak daha pahalı bir analiz olan akış-katı analizi tercih edilmemiştir. Yumuşak robotun hava ile doldurulması sırasında şekil

değişimini ve robotun hareketini üretmeden önce tahmin edebilmek üzere ABAQUS yazılımı kullanılarak lineer olmayan sonlu elemanlar analizi yapılmıştır.

Tasarım sürecince ilk adım robotun tahrik edileceği hava kanal yapılarını belirlemektir. Tasarlanan yumuşak robotun iki adet hava boşluğu bulunmaktadır, bunlardan birincisi hava ile tahrik edilecek ve yumuşak robotun genişleyip kubbe şeklini almasını sağlayacak olan hava kanalıdır. İkinci hava kanalı ise kubbe şeklini alan yumuşak robotun vakum kuvvetini oluşturacağı ve yapının altında bulunan hava kanalıdır. Bu çalışmada beş adet hava kanalı geometrisi seçilmiştir bunlar: spiral, semicircular, center spiral channel, circular channel ve vertical channel. Araştırmalar ve analizler sonucu hava kanalı geometrisindeki dairesel tasarım ne kadar fazla olursa o kadar fazla vakum kuvveti elde edildiği gözlemlenmiştir.

İkinci adım yumuşak robotun dış geometrisinin seçiminin yapılmasıdır. Dış geometrinin seçiminde doğada var olan yapılar göz önünde bulunarak araştırma yapılmıştır. Yapılan araştırmalar sonucunda geckonun adeziv fibrilleri ve ahtapotun kol modüllerinin yapısının tutundukları yüzeyde maksimum vakum kuvvetini oluşturduğu gözlemlenmiştir. Bunların yanı sıra ahtapotun kol modüllerinin yapısı yumuşak robotik sistem tasarımı için daha uygun olduğuna karar verilmiş ve yumuşak robotun dış geometrisi ahtapot kolunun basitleştirilmiş geometrisi olarak tasarlanmıştır. Yumuşak robotun hiper-elastik malzeme yapısı üzerinde daha çok kontrol sağlamak ve kubbe yapısını arttırmak için yumuşak robotun malzemesinden daha rijit bir malzeme olan kağıt tabakası, yumuşak robotun tahrik edilen hava kanallarının altına yerleştirilmiştir. Bu yöntem yumuşak robotun elastik malzeme yapısı sayesinde şişmesini, fakat daha rijit bir malzeme olan kağıdın eklendiği kısmın daha az deforme olmasını sağlayacaktır, böylelikle istenilen kubbe yapısı arttırılarak vakum kuvveti artacaktır.

Üçüncü adım yumuşak robotun malzeme seçimini yapmaktır. Yapılan araştırmalar sonucunda yumuşak robot imalat alanında kullanılan “Smooth-on” firmasının “Ecoflex 0030” modelinin yaygın olarak kullanıldığı görülmüştür. Malzemenin hiper-elastik yapıda olması ve hava ile şişirilip dayanıklı yapısı sayesinde yüksek deformasyonları kaldırabilmesi sayesinde yumuşak robot malzemesi olarak seçilmiştir.

Dördüncü adım yumuşak robotun yukarıda verilen tasarım ve sınır koşulları çerçevesinde üretimini yapmadan önce hareketinin tahminini ve oluşturacağı vakum kuvvetinin büyüklüğünü anlamak için sonlu elemanlar analizinin yapılmasıdır. Malzemenin yapısı ve geometrinin yüksek deformasyonlara maruz kalması analiz tipinin lineer olmayan analiz olmasına sebep olmuştur. Analizin en önemli sınır koşullarından biri, hava kanallarının yüzeyine basınç uygulanması sonucunda yumuşak robotun hava ile şişmesi modellenmiştir. Yapılan araştırmalar ve bu alandaki önceki çalışmalara bakıldığında akışkanlar dinamiği ile çözüm yönteminin sonuçlara etkisinin çok fazla olmayacağına karar verilmiş ve denge durumunda oluşacak vakum kuvvetinin önemi bu çalışmada daha önemli görüldüğü için hesaplamalı akışkanlar dinamiği çözüm yöntemi olarak seçilmemiştir. Beş adet seçilen hava kanalı tasarımlarında her bir model için dokuz adet analiz ile toplamda kırk beş analiz yapılmıştır. Vakum kuvvetini oluşturan iki temel parametre olarak kağıt kalınlığı ve kontak alanı seçilmiştir. Kağıt kalınlığının vakum kuvveti üzerindeki etkisini incelemek için üç farklı kalınlık belirlenmiş ve her bir model için uygulanmıştır. Diğer bir taraftan kontak alanının vakum kuvvetine etkisinin incelenmesi için üç farklı değer seçilmiş ve aynı şekilde her tasarım için uygulanmıştır.

Beşinci ve son adım olarak yumuşak robotun üretimi ve deneyi anlatılmıştır. Üretim yöntemi, sıvı silikonun üç boyutlu yazıcıdan basılmış plastik kalıplara dökülüp beklenmesi ile yumuşak robot üretilmiştir. Referans geometri olarak spiral hava kanalına sahip tasarım seçilmiş ve üretilmiştir ve deneysel olarak sonlu elemanlar modelinin doğrulanması bu model ile yapılmıştır. Deneysel olarak ise sonlu elemanlar analizinde uygulanan iç hava basıncı plastik hortum yardımı ile hava kanalı içine aktarılmış ve oluşan vakum kuvveti basınç sensörleri ile takip edilmiştir.

Yapılan analizler ve deneyler sonucunda, center spiral hava kanallarına sahip olan aktüatör diğer önerilen hava kanallarına göre daha fazla vakum kuvveti oluşturduğu gözlemlenmiştir. Kağıt kalınlığı ve kontak alanı etkisi incelendiğinde ise kağıt kalınlığının inceliği vakum kuvvetini olumlu yönde etkilerken kontak alanının azalması vakum kuvvetini azalttığı gözlemlenmiştir. Center spiral aktüatörün vakum uygulamalarında, insan robot etkileşiminin güvenli olması istenen uygulamalarda, sağlık alanında ve seri üretim hatlarında vakum ihtiyacını karşılamak amacıyla kullanılmasının faydalı olacağı sonucuna varılmıştır.





## 1. INTRODUCTION

Soft robotics is the subfield of robotics, which are made out of soft, highly flexible materials and can provide more degrees of freedom compared to conventional robotic applications. The mainstream design ideas in soft robotics come from nature and can be refer to as bio-inspired designs. The biggest objective of the soft robotics is to design, control, and manufacture of flexible structures, which can interact with humans with safer way. Although there are many challenges in soft robotics, they can be considered as lightweight and affordable structures as well as increased degrees of freedom (DOF) compared to conventional robotic systems. In order to manipulate and give a motion to soft robots, actuation methods are required such as pneumatic, thermal and electrically driven which are widely used methods in this field.

One of the first multi-gait soft robot is found by Shepherd et al. (2011) and it is shown in Figure 1.1, it is pneumatically actuated flexible walking soft robot, and it consists of five separate air tubes that feeding the four different leg and one body (middle section).



**Figure 1. 1 :** One of the Example of Multi-Gait Soft Robot. (Shepherd et al., 2011)

As it is shown in Figure 1.1, actuators could be consist of more than one segment. In the scope of this thesis, it is investigated that the design of soft pneumatic actuator (SPA) consist of single segment air cavity, which creates vacuum and suction force. The reason why a traditional suction pump is not used in this thesis is that sucking the air from soft robotic systems will cause buckling and collapse of the soft robot's

material when the air is deflated from the air channels. The main dominant factor in this case is the material, because of the flexibility and highly deformable material characteristic in pneumatic soft robots, vacuum pump like machines cannot be used in order to create suction force. Alternatively, positive pressure driven soft robot methodology is found more proper in this type of applications and hence air channels are filled with air then the vacuum is created under the geometry as shown in Figure 1.2-b. In contrast when the air channels is not inflated with air there is an atmospheric pressure in the vacuum cavity as shown in Figure 1.2-a. Moreover, when the air is inserted via air inlet to the air channels of soft robot, dome like structure will cause increased volume in vacuum cavity and finally suction force and vacuum will be created. In this study, it is decided to design five different air channel geometry and they are compared among themselves. In addition, numerical study conducted in ABAQUS software is validated with experimental study of the reference model. Besides the design variation of air channels, soft robots' outer geometry is bioinspired from octopus' arm, which can apply tremendous adhesive force to substrate.

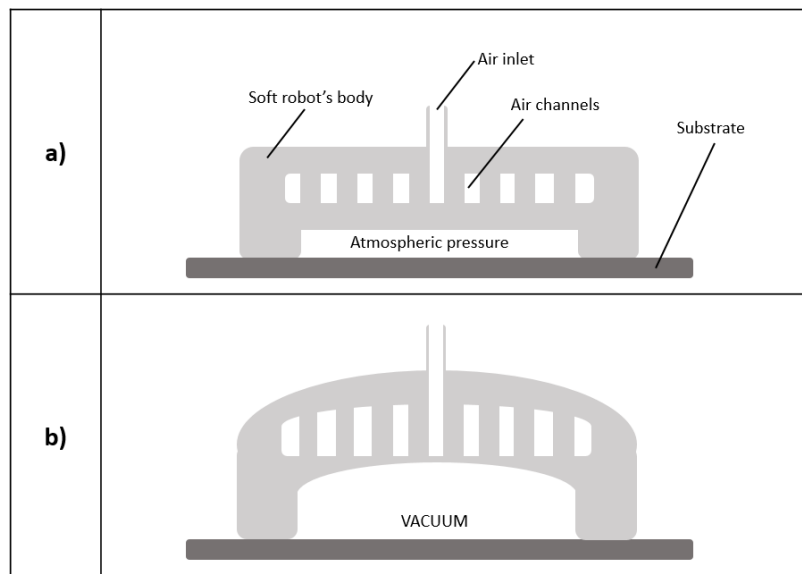


**Figure 1. 2 :** Schematic of the Soft Robot, a) Stationary, b) Inflated with Air.

The main parameters effect on the vacuum performance of soft robot is found that; air pressure inside of the air channels, material of the soft robot, inextensible layer that will provide more dome like structure and contact area between soft robot and substrate. Air pressure parameter is chosen as the maximum value that the soft robot can handle, inextensible layer is chosen as paper and it is clarified that the height of the paper has correlation with suction force. Moreover, contact area parameter effects

on suction force is investigated and it can be said that when the contact area increased vacuum performance of soft robot increases. In order to create more vacuum, suction force and predict the motion of mechanism, forty-five different nonlinear finite element analysis is done over five different soft robot designs and one reference model is validated with experimental work.

### **1.1 Purpose and Workflow of Thesis**

Production and testing system of real-life applications can be considered as expensive and time-consuming procedures. In order to reduce time and cost in engineering and academic applications, numerical analysis is used with the help of improved computational power. In more detail, motion of soft robotic system, which is made of hyper-elastic materials, can be predicted by FEA. It is better to use FEA before manufacturing the soft robot and testing the different designs in computer environment. Main aspire of this study is to address the design parameters that affect suction force of soft robotic system and manufacturing of it. Five different air channel geometry is used in the design of soft robot, which includes the parameters such as the height, length, distance to bottom and top surface of body and finally volume of air channels. Outer shape design of soft robot is inspired from octopus' geometry, which has satisfactory adhesive force on substrate that is holding on.

Complete soft robotic research workflow is highlighted in Figure 1.3, which includes four main steps such as the 3D design of geometry, manufacturing of the prototypes, testing and validation of the numerical models with experimental results, and finite element model results of untested actuators. After all these steps, measured results can be compared with the simulation results, then one can assume the FEA model is suitable and might be used for further studies. In this study, only one soft robot is manufactured and validated as shown in Figure 1.3, which is called spiral design and other four designs are only simulated with FEA.

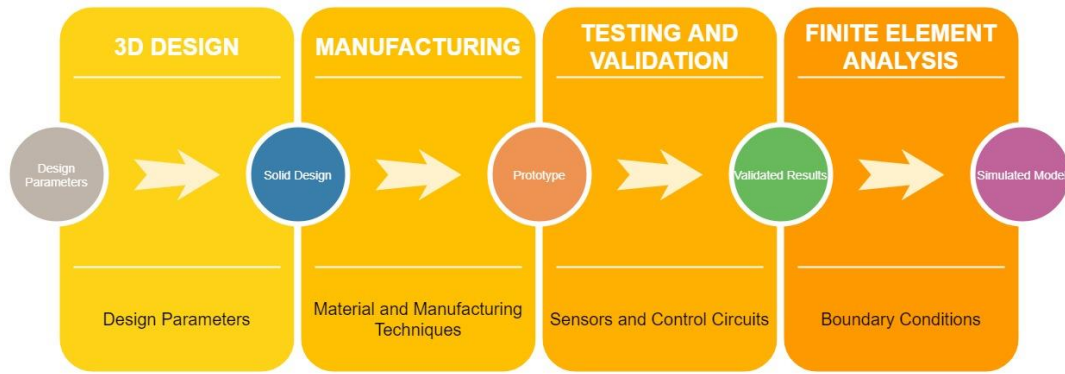


**Figure 1. 3 :** Workflow of Soft Robotic Research.

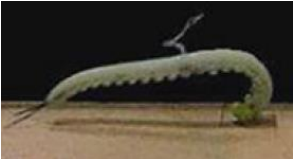
## 1.2 Literature Review

Emerging research area of soft robotic has been investigated in the last years. It is mentioned in the study from Bao et al. (2018), article related to the soft robotics started to be published from 1990, in addition, contribution to the soft robotics literature of the countries in the world from 1990-2017, United States is stated the rank 1 whereas Turkey is rank 17. In this section, general history of literature, numerical studies, experimental works, and material developments, design, manufacturing and testing of soft robotic literature will be given.

A study conducted by Çivici and Parlak (2020) has shed some light on the description of soft robotic systems that have the highly flexible materials and DOF while performing the grasping, crawling and manhandling. Although soft robotics have being considered an area at its infancy years, it is mentioned in the article Laschi, Mazzolai, and Cianchetti (2016), soft robotics academic publications was at almost 1000 in 2016 whereas it was close to zero in 2004. For example one of the first study can be given on soft robotic hand, published by Noritsugu, Takaiwa, and Sasaki (2008), it is said that in the article, pneumatically driven five artificial muscle finger is created and the aim was assisting the bending motion and to increase the grasping of hand. Another leading article on soft robotics from Rafsanjani, Zhang, Liu, Rubinstein, and Bertoldi (2018) presented a soft robot, which is inspired from snake's skin and takes advantage of Krigami Japanese paper cutting art, they have proved that when the surface skin of snake imitated and wrapped around a soft robot, it can propel itself. According to Laschi and Cianchetti (2014) the latest improvements in soft materials, configurable designs and non-linear modeling capability of the systems have increased the interest about soft robotics.

When it comes to application areas of soft robots, wide range of examples can be given from space exploration to search and rescue. Onal and Rus (2012) have mentioned on their article about the possible application areas of soft robotics could be classified as safer human interaction, assisting to humans by means of artificial muscles, and wearable soft interfaces. In addition to the specific application areas, Trivedi, Rahn, Kier, and Walker (2008) briefly mentioned in a study, which says, soft robots could be used for sensitive assignments in unstructured environments. Moreover, article presented by Lee et al. (2017) mentioned about the medical and surgical application areas of soft robots because of their compliant mechanism designs and increased DOF. Some real life examples and details of soft robots are given below in Table 1.1.

**Table 1. 1 : Real Life Example of Soft Robotics.**

Soft Robot	Design	Inspiration	Actuation Method
Multi-gait (Shepherd et al., 2011)		Starfish	Pneumatically
Octopus Robot (Laschi et al., 2012)		Octopus	Shape memory alloy (SMA)
GoQbot (Lin, Leisk, & Trimmer, 2011)		Caterpillar	Anterior and posterior flexors

Soft robotic systems usually consist of bio-inspired designs from nature, study done by Rogó , Zeng, Xuan, Wiersma, and Wasylczyk (2016) investigated caterpillar locomotion and kinematics, it has been noted that caterpillar is used for inspiration for the design of their actuator. Also, Seok et al. (2013) had conducted a bio-inspired soft robot study; they have developed a soft robot, which takes inspiration from mesh worm by means of peristaltic motion. An octopus inspired soft robot prototype is done by Calisti, Corucci, Arienti, and Laschi (2015) and noted that dynamic model is set-up

with the help of evolutionary techniques. Classical robotic systems have been designed with the help of computer-aided-design (CAD) software, as mentioned in the article Rus and Tolley (2015). However, conventional CAD programs cannot predict the complex motion characteristics of soft robots. Study conducted by Taylor (2013) highlighted problems of soft robot design and categorized as morphology (shape of soft robot), material and locomotion, which are directly related to each other in addition they proved that evolutionary algorithms for instance genetic algorithm (GA) can be used to generate soft robot designs automatically.

In order to model the highly non-linear material of the soft robots', proper hyper-elastic material models should be used for instance Yeoh, Ogden, Arruda-Boyce, Polynomial, and Van-der-Waals models as it is proposed by Agarwal, Besuchet, Audergon, and Paik (2016). In the same study conducted by Agarwal et al. (2016), mentioned that when performance and characterization of SPA considered in steady state, fluid-flow dynamics into the fluid channels of soft robot is not taken into account. It is also said in the article conducted by Du Pasquier, Chen, Tibbits, and Shea (2019), when the steady-state results are the focus of the interest, transient effects of airflow could be neglected. Besides that, article from Qiao, Wang, Jeong, Rodin, and Lu (2017) substantiates the fact that Agarwal et al. (2016) mentioned previously about unnecessary calculation of fluid-flow dynamics in a steady state condition with the assumptions such as isothermal process, air is an ideal gas and no leakage occurs in the process. A follow-up study from the same team conducted a research about suction force created by craters, both numerical and experimental works conducted L. Wang, Ha, Qiao, and Lu (2019). In the same study it is highlighted that for the simulation part, ABAQUS software is used and more specifically \*FLUID CAVITY module is used in the FE model in order to calculate the suction force and cavity pressure. It is concluded from the both articles, to calculate the volume and pressure change in a closed area, ABAQUS and \*FLUID CAVITY module can be used. It is explained in the manual of ABAQUS that ("About surface-based fluid cavities", 2020) fluid cavity module controls the relationship between cavity volume and pressure.

Another article presented by Iida and Laschi (2011) says that robotic systems mostly composed of structural materials for instance steel and aluminum whereas soft systems infrequently consist such rigid materials, besides they usually take advantage of soft and flexible materials. According to a study Lee et al. (2017) soft robot's materials

mostly selected as rubber or silicone, the reason behind this selection is mentioned as the soft structural systems should be able to carry out flexible motions and material's elasticity modulus is mostly in between  $10^4$ - $10^9$ . In addition to the rubber and silicone, material selection of soft robots directly related to the actuation methods such as stimuli responsive actuation with the help of (SMA) or soft-rigid hybrid systems, which takes advantage of both soft and rigid components for combining high precision and human interaction Schmitt, Piccin, Barbé, and Bayle (2018). To generalize the actuation methods, one study put forward three methods such as; variable length tendons, fluidic actuation and electro-active polymer based (EAP) (Lee et al. (2017)). In addition to the actuation methods, when choosing a material for soft robotic system, prediction the effects of material is important. It could be said that in order to predict and validate the material behavior, (FEA) and experimental study is necessary. As a comparative example, Mosadegh et al. (2014) experimented both Ecoflex 00-30 and Elastosil for extensible layer whereas Polydimethylsiloxane (PDMS) and paper is used for inextensible layer respectively as illustrated in Figure 1.4.

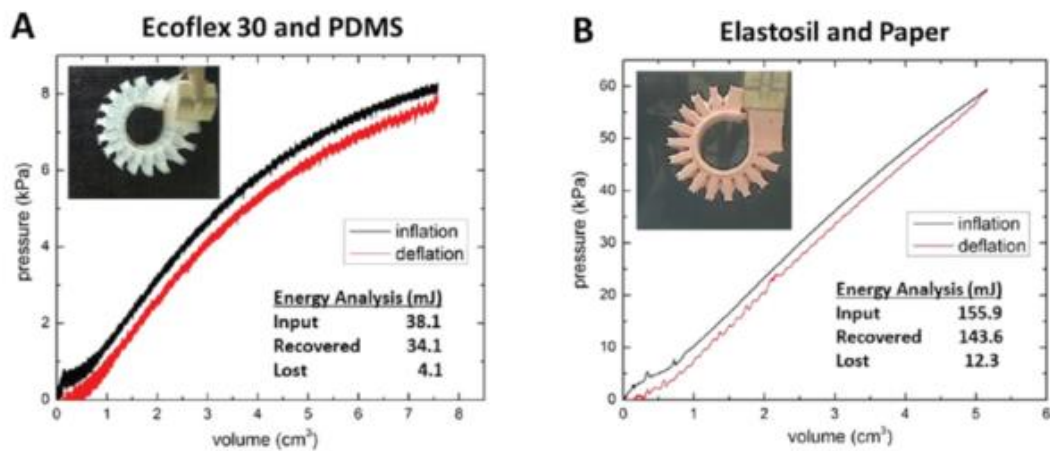


**Figure 1. 4 :** Effect of Material on volume-pressure curve. (A) Extensible material of Ecoflex 30 and inextensible layer of PDMS, (B) extensible material of Elastosil and inextensible layer of paper is used. (Mosadegh et al., 2014)

Moreover, Agarwal et al. (2016) mentioned in the article that they observed soft robotic actuators formed from Ecoflex 00-10 and Ecoflex 00-20 is not to be as durable as those manufactured from Ecoflex 00-30 because of the mechanical properties.

For the manufacturing side of the soft robotic systems new technologies are emerged comparing to conventional methods. Schmitt et al. (2018) mentioned in a study, methods to produce a soft robotic system could be given as molding, 3D printing, thin-

film fabrication, shape deposition and bonding. As an example of molded soft robotic actuators, Agarwal et al. (2016) highlighted that the actuator consists of single air cavity and manufactured in a one-step molding production. In addition, inextensible layer is bonded on the surface of actuator and it helps to bend and inflate only to desired direction. According to a study conducted by Majidi (2014) methods such as soft-lithography, roll-to-roll, and 3D printing is used widely in manufacturing of soft robotics. In addition, laser micromachining, computer numerical control (CNC) milling, and 3D printing methods provide cheap and easy customized manufacturing processes as well as reduced production costs.

For the testing and control methodology of the soft robotic systems, pressure control of the actuator plays an important role. One study conducted by Elsayed et al. (2014) proposed a pressure controlling methodology that is based on solenoid valves. Actuator used in the study composed of three separated air channels, and each of airline is controlled with solenoid valves. Hence, pressure is supplied with air compressor and desired pressure is controlled with valves. Another study conducted by Digumarti, Conn, and Rossiter (2017) set-up an experimental without a solenoid valve, instead pressure is measured with an external pipe which is connected to the actuator body. In this way, pressure measured inside of the actuator is used in the finite element analysis models, which the pressure value is applied into the walls of the actuator.

In a study presented by Yang (2013) mentioned about a robotic system, which is called “in-pipe robot”, could be used for investigation of the inner surface of the pipe. It has been proven in study two different air channeled soft robots can be used as “in-pipe robot” to search water networks underground. Methodology explained in the study is “positive pressure actuated suction-cup (PPAS)”, using the compressed air to actuate and create suction force from soft robot rather than applying vacuum to the air channel. Another similar study is conducted by Tang, Zhang, Lin, and Yin (2018) investigated a “load-carrying Amphibious Climbing Soft Robot (ACSR)”. Similar to the study from Yang (2013) they aimed to design and manufacture a soft robot that creates vacuum and suction force, besides they used the soft robot for climbing and load carrying applications both underwater and ground.

## 2. ADHESION AND SUCTION FORCE PHENOMENA

### 2.1 Adhesion Mechanisms

Adhesion is a pulling process between different substrates that cling together after bonding of the surfaces cohesion occurs among similar molecules. More clearly, cohesion stands for tendency of similar surfaces to cling together for instance liquids with surface tensions have high cohesion forces. Various types of adhesion theories can be given but most important theories are shown in Figure 2.1 (Joo and Baldwin (2010)).

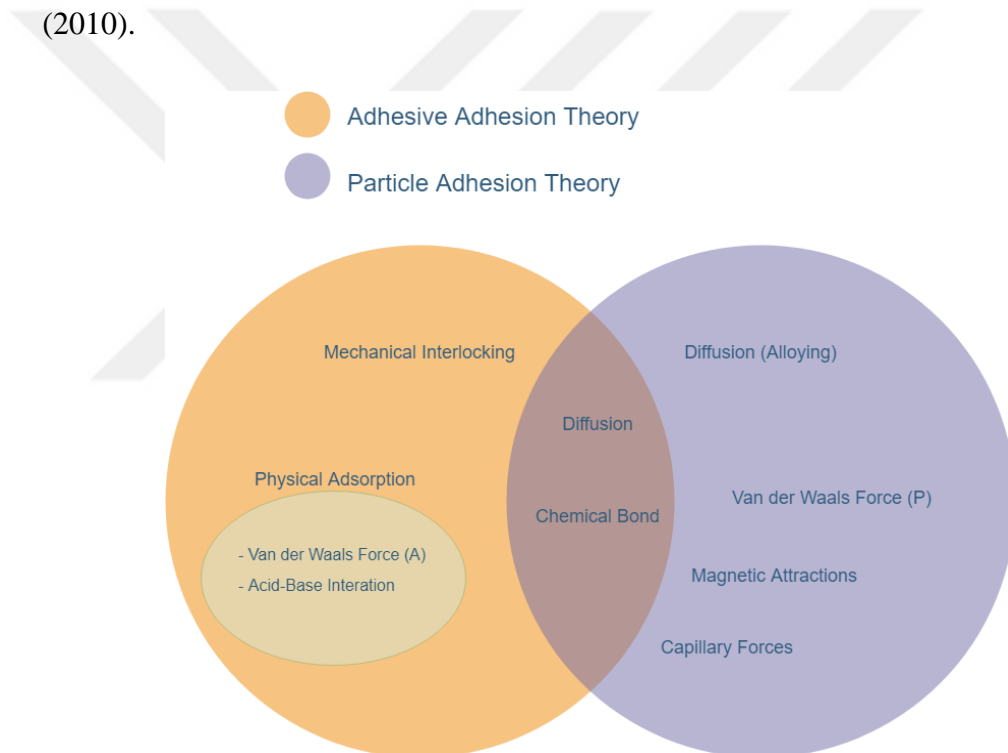


**Figure 2. 1 :** Classification of Adhesion Types.

The main adhesion mechanisms could be categorized into adhesive adhesion and particle adhesion. Mechanical interlocking could be explained as; adhesive materials fill the gaps and empty spaces of surfaces and engage the surfaces together. Whereas, when the particles and molecules of some substrate materials are remote and soluble in each other, they might unite by diffusion. An illustration is given to mechanical interlocking shown Figure 2.2 adhesive penetrates into the holes and locks to the substrate.

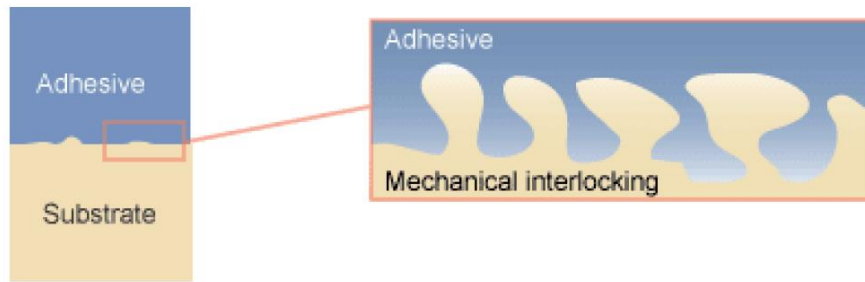


**Figure 2. 2 :** Adhesion Mechanisms. (Bhuse, 2018)

Van der Waals forces are general definition used to clarify the attraction of molecular forces between molecules. Van der Waals forces in the adhesive adhesion (A) and particle adhesion (P) are different because of force between straight surfaces in contact is not similar between a round particle and flat surface with respect to effect of surface hardness.

Similar to these mechanisms force that occurs is called adhesive and cohesive forces. Adhesive and cohesive forces are related with macroscopic properties. Cohesive forces can be explained as molecular forces that occurs between same substrate molecules, which is responsible of property of liquids resisting disconnection.

## **2.2 Suction Mechanism and Suction Force**

Suction can be described as a force that produce vacuum on solid, gas or liquids. When the air is sucked from a specific volume or space, it results in a pressure drop. Pressure difference relative to the atmospheric environment creates the suction force, the more negative pressure inside the cavity, more the suction force occurs. Suction cups, vacuum cleaners, vacuum pumps and breathing processes can be given to examples for suction mechanisms. For a specific example, suction cups can be used to adhere to substrates without any given damage.

### **2.2.1 Suction cups**

Suction cups are objects that are used to hold and suck to substrate surfaces by using negative fluid pressure inside of the cavity and creating partial vacuum inside of it. They are mostly manufactured from flexible materials and their design is inspired from nature such as octopuses and squids. There are two types of suction methods on substrates and they are shown in Figure 2.3.

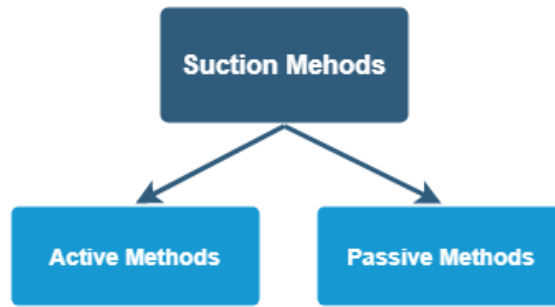


**Figure 2. 3 :** Suction Methods in Suction Cups.

Active suction cups should be actuated continuously with vacuum pump in order to maintain the suction force on surface. Usage of active suction cup applications involve pump and thus the system weight increases. On the other hand, passive suction methods are not require vacuum pump and their applications both lightweight and quiet. However, bonding and debonding processes are not easy to control in passive suction cups compared to active methods (Ge et al., 2015). Typical operation and working principal of a suction cup consist of steady phase, pushing phase, adhere phase, and detached phase, process is shown in Figure 2.4.

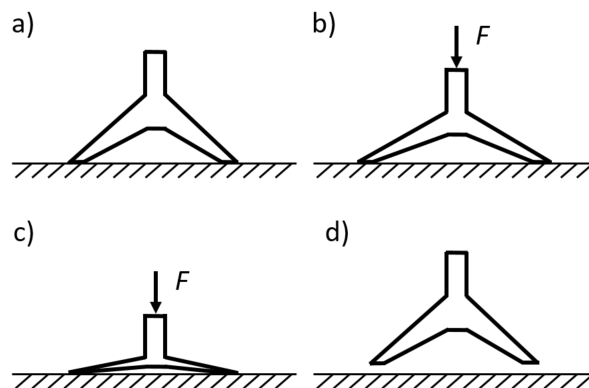


**Figure 2. 4 :** Working Operations of Suction Cups, (a) Steady phase, (b) Pushing phase, (c) Adhere phase, (d) Detached phase.

In the steady phase, the suction cup is placed on the substrate without any external force. After applying an external force due to the flexible material characteristics of the suction cup, it deforms and enters the pushing phase. While the air inside of the inner cavity squeezed out, negative pressure inside of the cavity under suction cup increase due to the volume change. In adhere phase, suction cup is pressed onto the surface as much as possible to create maximum suction force and negative pressure

inside of the cavity. If the external force pulls the suction cup, it enters detached phase until the sealing is broken with the surface.

### 2.2.2 Bio Inspirational design

Suction cups are bio-inspired from octopuses with respect to working mechanisms and designs, which have the ability to attachment and detachment onto objects with powerful muscle contacts in the arms. In a study conducted by Sareh et al. (2017) showed the details of octopuses suction module and it is given in Figure 2.5.

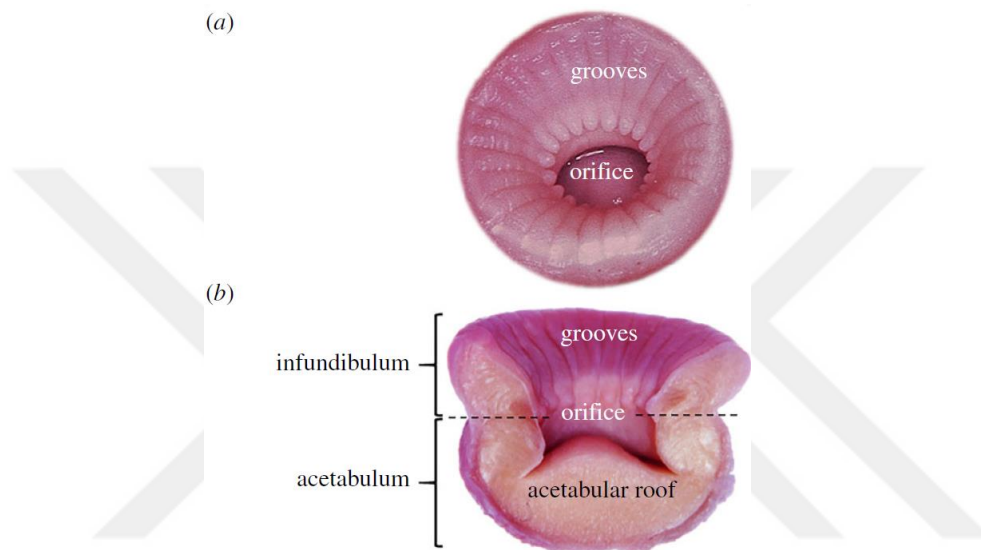


**Figure 2. 5 :** Octopus Sucker, (a) View with grooves and orifice, (b) Cross section of sucker. (Sareh et al., 2017)

Octopus sucker contains two major parts, infundibulum and acetabulum namely. Infundibulum is the soft and flexible part of the octopus whereas acetabulum is more rigid and elliptic part of the octopus sucker. When the octopus sucker touches on a substrate infundibulum becomes flat and takes the shape of the substrate surface with the help of its flexible material characteristic. The rims at the bottom surface of the infundibulum provide sealing. Then acetabulum narrow itself with the help of radial muscles and decrease the inner pressure inside of the sucker. Suction cups are mostly designed to work like octopus sucker, they are decreasing the volume and increasing the negative pressure inside of the inner cavity as it happens in octopus sucker.

### 2.2.3 Physic and calculation of suction mechanism

Physics behind the working mechanism of the suction cup can be explained with pressure difference principle. Once the inner pressure become less than atmospheric

pressure, vacuum occurs thus suction force. Parameters that effect the suction force are atmospheric pressure, surface roughness of substrate, material of the suction cup, payload force that applied onto the suction cup.

Assumptions that is being done while calculating the suction force:

- No air leakage occurs while attachment and detachment process
- Air flows out from the inner cavity of the suction cup
- Operation is isothermal and ideal gas assumption is valid for air

Figure 2.6 shows the main calculation principles while the attachment and detachment processes of the suction cup.

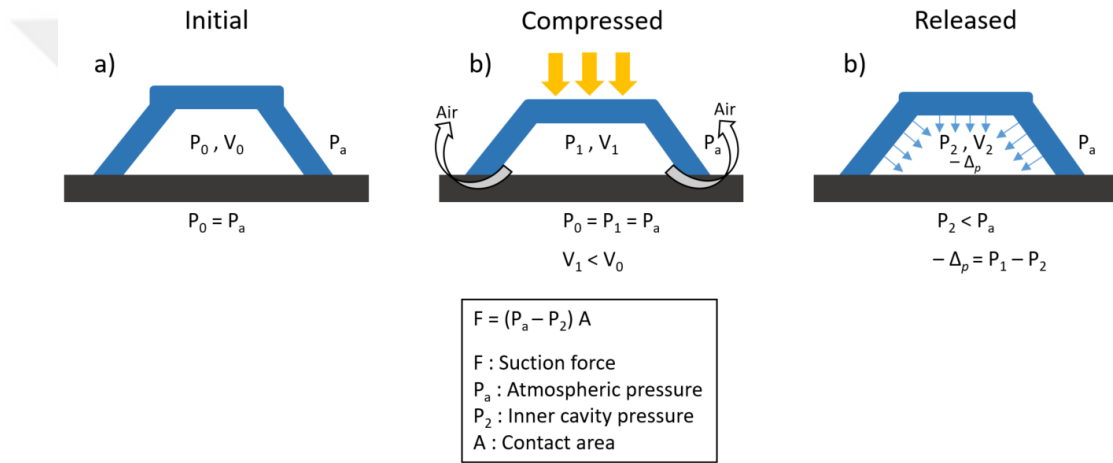


**Figure 2. 6 :** Suction Force Calculation.

As it is shown in the Figure 2.6, suction force is dependent on pressure difference between atmosphere and inner cavity as well as contact area. In the initial position without any preload, suction cup is at steady state phase, sealing is not ensured and inner cavity pressure is equal to the atmospheric pressure. With the assumptions that are mentioned above, fluid dynamics is regarded as in equilibrium and it is suffice to calculate the suction force and simulate with continuum solid mechanics.



### 3. DESIGN OF SOFT ROBOT

As it mentioned before, in this study octopus sucker is imitated in the design of soft robot due to its extreme suction force creation ability. Mainly there are three important geometrical sections of soft robot. First, outer shape of soft robot is designed as cylindrical to make radial expansion and deformation, and second, inner cavity designed to create dome shape when the soft robot is inflated with compressed air. Lastly, air cavity designs are chosen to obtain radial expansion as much as possible. Yang et al. (2013) mentioned in a study that spiral design of air cavity is more likely to connect the channels via a spiral geometry. One another example can be given from Tang and Yin (2018) they have proved in their study that octopus inspired suction cup, doming actuator, can be used as an adhesion actuator as switchable. Schematic representation of the soft robot with its important sections is shown in Figure 3.1. Main purpose is to find a design parameter set, which gives the best vacuum performance.

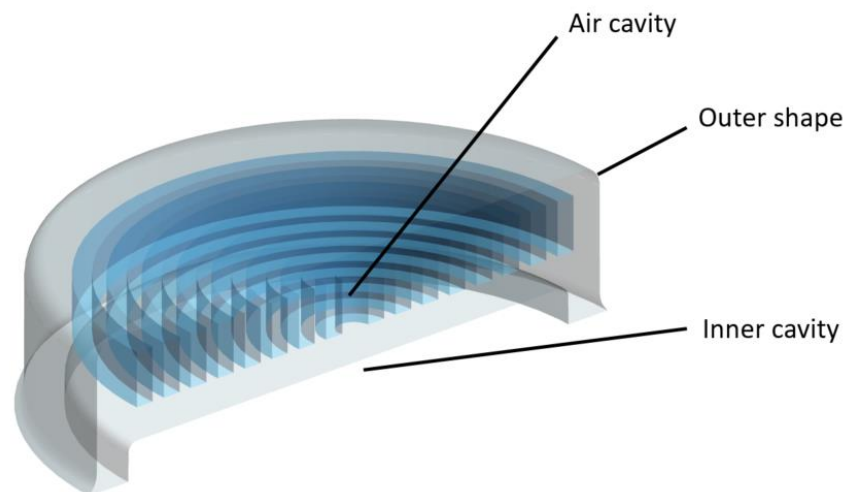


**Figure 3. 1 :** Schematic Representation of Soft Robot.

#### 3.1 Soft Robot Segmentation

In this study, it is decided that fixed outer geometry will be used and five different air cavity designs are chosen in order to create radially deformation and dome shape. Same outer shape for all soft robot not only helps to differentiate the vacuum

performance, but also enables to identify only the important parameters that effects the vacuum performance. Although air cavity designs are different, their cross sectional area is chosen the same rectangular shape. To conclude, five different soft robot designs will be evaluated and one will be chosen the best result driven design, and in Figure 3.2, cross section of soft robot designs are shown namely spiral, semicircular channel, center spiral channel, circular channel, vertical channel is shown. Spiral design is proposed by Yang et al. (2013) is selected to verify the results given in the study and to derive the other four unique design in this study. As it is mentioned, four unique designs are proposed in this study namely: semicircular, center spiral, circular and vertical channel. As it is mentioned before, the main considered methodology to choose the four unique air cavity design is to create radial deformation and to increase the diameter of the soft robot as much as possible. Hence, this will create the dome shape and vacuum under the soft robot.

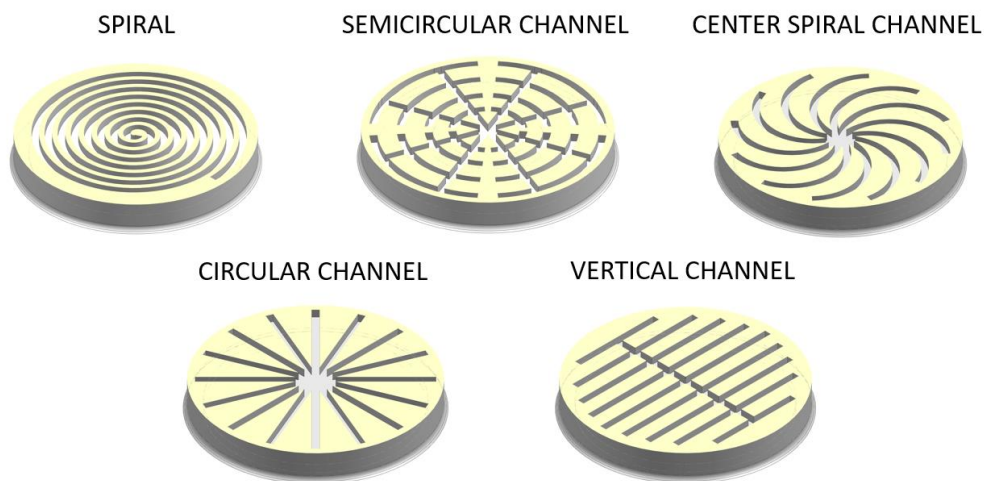


**Figure 3. 2 :** Cross Sectional View of Five Soft Robot Designs.

All air cavity designs will be evaluated and compared to each other by using finite element analysis. Vacuum performance will be calculated with both analytical and finite element analysis. In this study, soft robot with spiral design is chosen as the reference model and used to validate the FEA simulation. Spiral channel design is chosen due to its diameter increases radially from center to outer and expected to create expansion both radially and vertically. Other air cavities are chosen in order to differentiate the spiral channel and the best vacuum performance will be chosen among them. Different air cavity cores is shown in Figure 3.3.

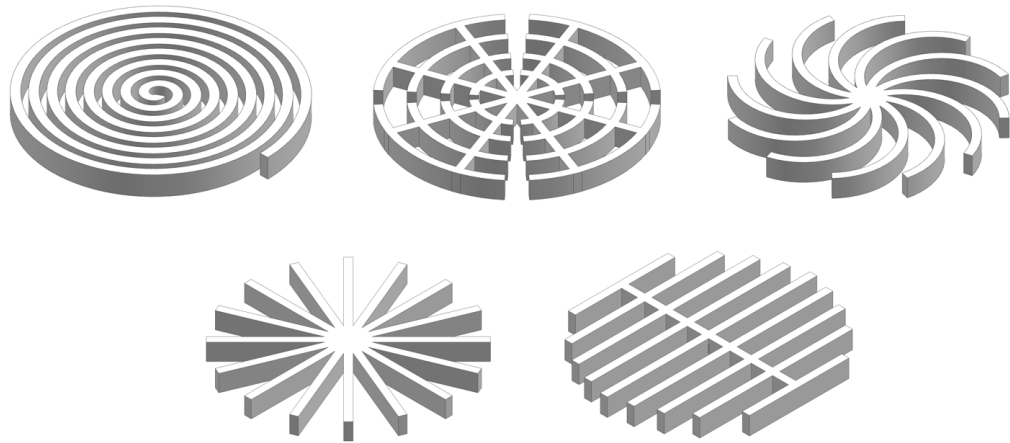


**Figure 3. 3 : Air Cavity Designs.**

Even the main consideration for design selection of air cavities is to create more vacuum under the inner cavity, it is also considered the manufacturability of the air core for instance with the help of additive manufacturing.

### **3.2 Design Parameters**

In order to compare the relations and see the evaluation of the design process, parametric design study is conducted and the best vacuum performance will be chosen among them. Most important five parameters are chosen with respect to their effect for vacuum performance and manufacturability. They are shown in Figure 3.4, namely a, b, c, d, and e. Configurations for the dimensions that are illustrated in Figure 3.4 is: in any case, dimension of “a” should be higher than dimension of “c”, and the dimension of “d” should be smaller than the dimension of “e” as it is mentioned in the article written by Tang et al. (2018) they have proved that, maximum shear force is obtained when the dimension of “d” smaller than “e”, hence the vacuum performance of the actuator. It is also explained that the thin top surface wall thickness helps to bend as dome shape for the soft robot. Some parameters are taken as fixed parameters such as “a” = 32 mm, “b” = 33 mm, “d” = 2 mm and “e” = 3 mm. Main reason to choose “b” bigger than “a” with the amount of 1 mm is to mimic the octopus’ infundibulum as it is shown in Figure 2.5. Dimension of “d” and “e” is chosen Dimension of “h”, which represents the paper height, has three values and it varies with contact area, which depends on the dimension of “c”. Values of “h” is 0.5 mm, 0.3 mm and 0.1 mm. Similar to h, dimension of c has three values as well and they are 30 mm, 28 mm and 26 mm which helps to calculate the contact area of soft robot.

Difference between dimension of “a” and “b” effects the manufacturability, even if it is not directly related to the vacuum performance it is considered as a design parameter as well. In addition, for these design parameters, inextensible layer (strain limiting layer) is also highlighted as h in Figure 3.4 and the thickness of this layer is considered as a design parameter as well.

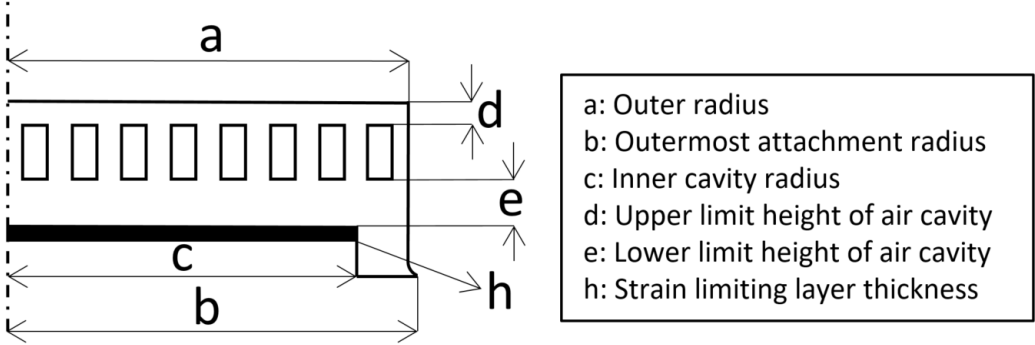


**Figure 3. 4 :** Design Parameters.

In addition, the design parameters shown above, air cavity cross section is parametrized and it is chosen as rectangular shape. The reason to choose rectangular shape rather than square is when the air is inflated into the channel, rectangular shape more likely to have bended and axial displacement, which is most likely to create dome shape. Cross section deformation schematic and design parameters are shown in Figure 3.5.

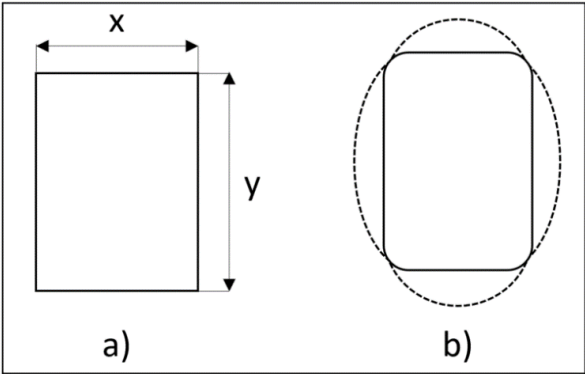


**Figure 3. 5 :** Cross Section of the Cavity, a) Before inflation, b) After inflation.

It is highlighted in Figure 3.5, a) presents the main cross section of air cavities and in this study dimensions are fixed into  $x = 2 \text{ mm}$  and  $y = 5 \text{ mm}$  respectively with the reason of minimum wall thickness requirement to manufacture the soft robot. Moreover, in the right hand side, b) represents the inflated cross-section of air cavity.

### 3.2.1 Parameters effect on vacuum performance

In addition to the all parameters explained above, it is concluded that there are some parameters that have an effect on vacuum performance. As it is mentioned before, in order to create vacuum in the inner cavity, there should be pressure difference between the air cavity and atmospheric pressure and it can be said that, more the pressure difference, higher the vacuum performance. Consequently, parameters that have an effect on vacuum performance is highlighted in the Table 3.1.

**Table 3. 1 :** Parameters that affect the vacuum performance.

Parameter	Unit (SI)
1. Air cavity pressure	MPa
2. Contact area	mm <sup>2</sup>
3. Strain limiting layer thickness	mm
4. Dimension of “d”	mm
5. Dimension of “e”	mm
6. Cavity geometry	-

Unit system is shown in the Table 3.1 chosen as International System of Units (SI). It is decided that six different parameters have the impact on vacuum performance and these parameters will be used to differentiate and find the proper design to create vacuum.

### 3.2.2 Parameters used in calculations

In order to calculate the suction force theoretically and compare the results with both experimental and numerical studies, theoretical hand calculations are necessary. In this sub-section, parameters that is used in hand calculations are given. For instance, to calculate the contact area equation 3.1, 3.2, and 3.3 is given as:

$$F_s = A \Delta P \quad (3.1)$$

$$F_s = \pi (b^2 - c^2) \Delta P \quad (3.2)$$

$$F_s = \pi (b^2 - c^2) (P_{atm} - P_c) \quad (3.3)$$

Where  $F_s$  represents the suction force,  $\Delta P$  is the pressure difference between atmospheric pressure ( $P_{atm}$ ) and inner cavity pressure of soft robot ( $P_c$ ), and finally

dimensions of “b” and “c” as its shown in Figure 3.4, indicates the outer and inner contact diameters respectively and resulting calculation of A represents the contact area. It can be concluded that from the equations given above, the more the differences between dimensions of “b” and “c”, higher the suction force will be. Although there is a dependency between the air cavity pressure (Table 3.1) and suction force, material characteristics of the soft robot constraints the air pressure level that is sent to the cavity.



#### 4. EXPERIMENTAL STUDY

In this section, the experimental study will be discussed with details about how it is conducted, what are the steps of it, and the methodology used. First, manufacturing methods of the selected soft robot design will be explained, and then the set-up of the experimental study will be given with the details of electronic circuit, electronic components, pneumatic components, programming and data visualization. Lastly, control and testing of soft robot will be explained for the selected reference model design.

Spiral design of soft robotic actuator is selected as reference model with the parameter combination of 0,1 mm paper height and 1290-mm<sup>2</sup> contact area, to use in experimental study and validation of the FEA model later on. Spiral air channel design of soft robot firstly conducted by Yang et al. (2013), and the later on Tang et al. (2018) studied the same geometrical design with different outer dimensions and methodology to create a climbing soft robot and vacuum actuator. To do the comparative work with the previous studies, it is decided to use spiral design in experimental study to validate the FEA model. Methodology used in experimental study and the systematic procedure is given in Figure 4.1.

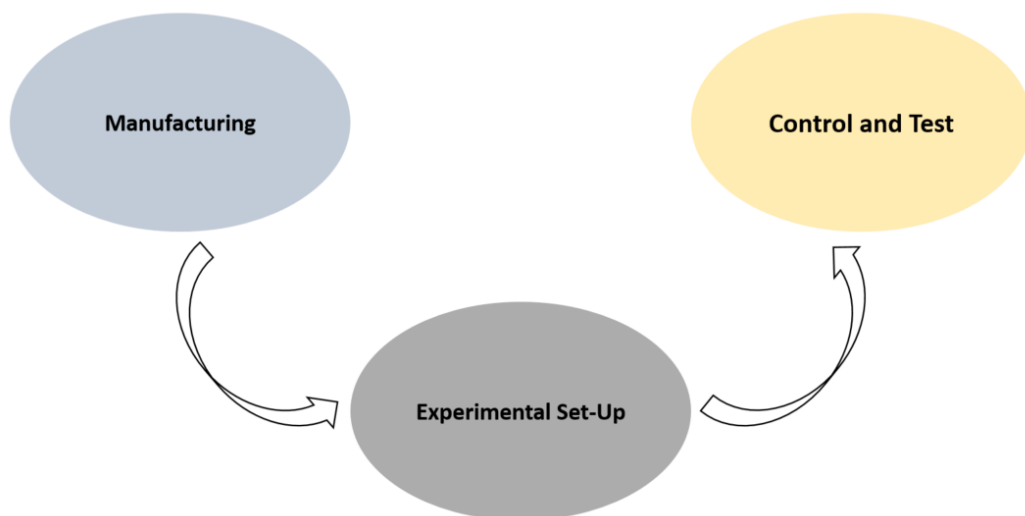


**Figure 4. 1 :** Process of Experimental Study.

## 4.1 Manufacturing Methods

The first step in the process of experimental study is to manufacturing the soft robotic actuator and in this section manufacturing steps of the spiral design of soft robot will be explained with the details of selected materials, tools that are used in manufacturing, and methods used in the processes. To manufacture the soft robot, three main steps are listed as:

- Preparation of the base material
- Manufacturing the plastic molds and molding the silicone rubber
- Assembly of the separate parts

Schematic representation of the manufacturing steps of the actuator is shown in Figure 4.2 starting with the base material preparation and ending with the complete assembly.

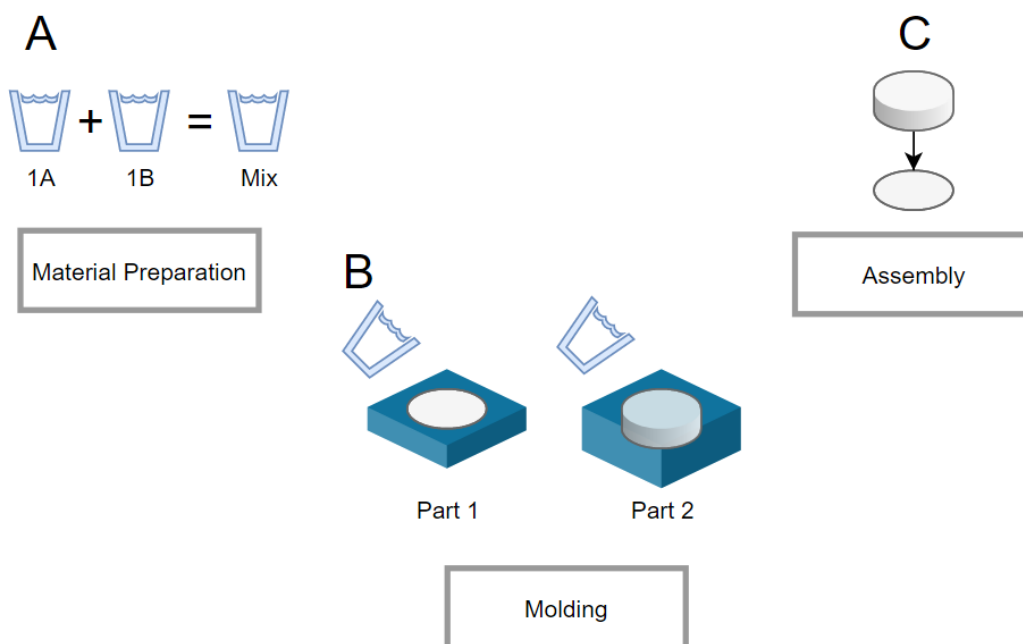


**Figure 4. 2 :** Representative Manufacturing Process of the Soft Robot.

Due to material details used in soft robotics are explained in the literature review, only the selected material details will be given in this section. There are two material selections to manufacture the soft robotic actuator. First, Ecoflex 0030 (Smooth-On Inc.) is selected as the base material to manufacture the soft robot and secondly, paper is used as inextensible layer (strain limiting layer). First Ecoflex liquid silicone rubber is mixed with equal amount of 1A:1B as shown in Figure 4.2-A, and mixture of the

liquid silicone is poured into the plastic molds to produce the bottom side of the design. Methodology used in Figure 4.2-B is called gravity molding and poured mixture in the mold is cured at room temperature for four hours. Then cured silicone is demolded from the bottom mold and silicone bottom part is placed on the top mold, which consist of liquid silicone as shown in Figure 4.2-C. Bottom part is placed on liquid cover on purpose to prevent sealing problems.

In order to prepare the mixture of the material, first part A and part B is mixed with equal amount of weight, 12.95 gram as shown in Figure 4.3, yellow box represents the part A and blue box is the part B of the silicone rubber, they are poured into separate plastic glasses and mixed. It should be noted that mixture is stirred for ten minutes paying attention not to create air bubbles inside of the mixture to prevent air gaps inside the cured silicone.

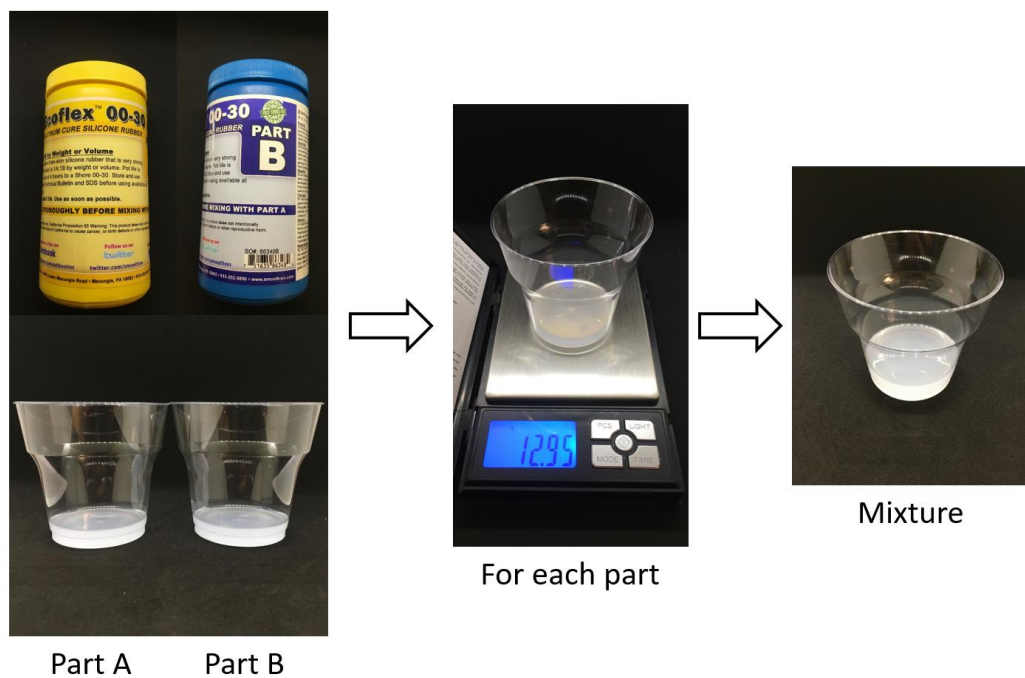


**Figure 4. 3 :** Material Preparation (Ecoflex 0030, Smooth-On Inc.)

For the mold production, conventional 3D printer is used with PLA material. Four main plastic molds are manufactured which they are air channel mold, air channel holder, bottom mold, and top cover mold respectively. Molding processes and parting line concept details are shown in Figure 4.4 schematically. Air channel mold is shown as number 1, bottom mold is number 2, and air channel holder is number 3.

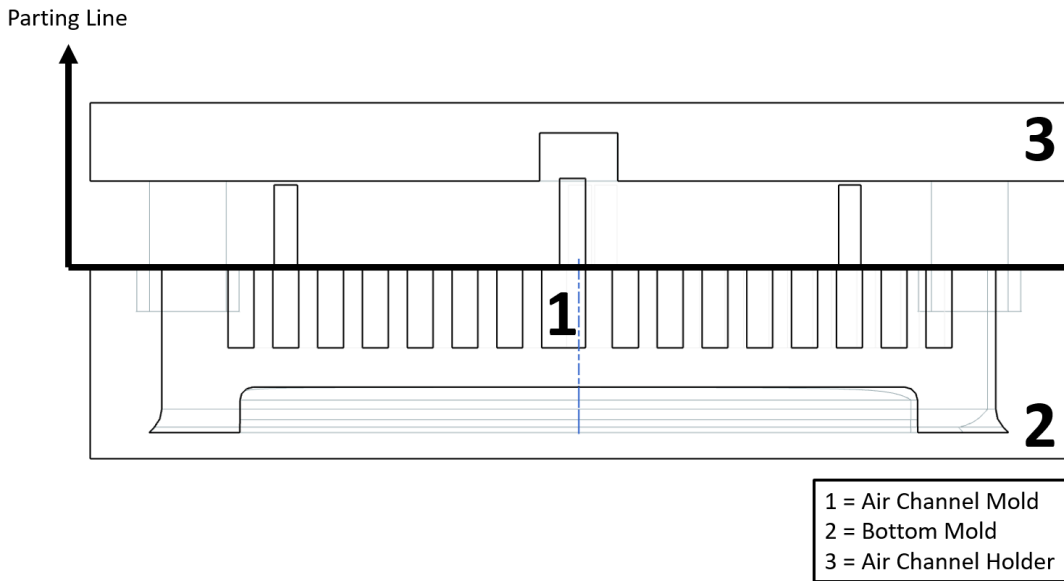


**Figure 4. 4 : Molding Techniques of the Spiral Design.**

Four manufactured plastic molds and 3D models are shown separately in Figure 4.5. Air channel mold is the part 1 in Figure 4.4 and it is used to create air cavities in the design. Bottom mold is the part number 2 in Figure 4.4 and it provides the outer geometry of the actuator. When the actuator is demolded from bottom mold, top cover mold provides the top surface of the actuator.

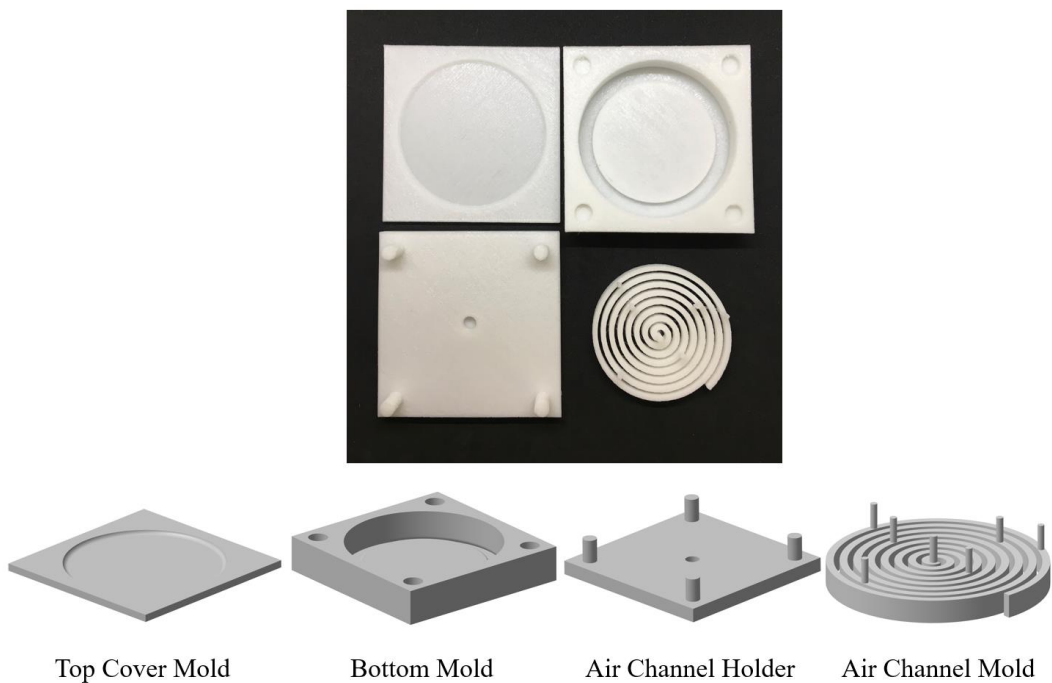


**Figure 4. 5 : Manufactured Molds and Part Details.**

After pouring the liquid silicone into the bottom mold, air channel mold which is assembled on the air channel holder, is placed onto the bottom mold with the help of four pins located in each corner, two-step processes is shown in Figure 4.6.

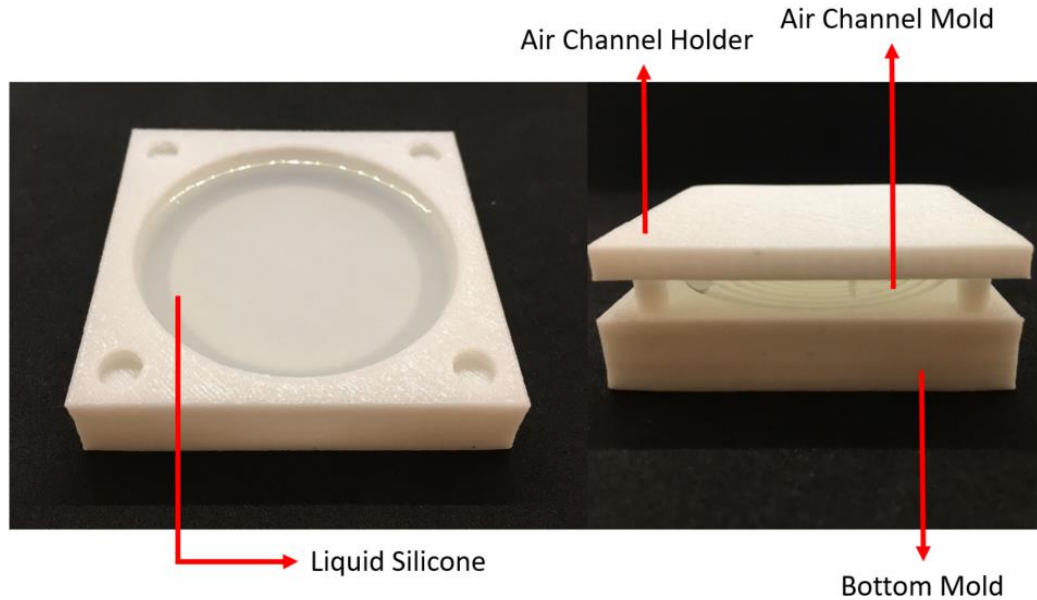


**Figure 4. 6 :** Molding of Bottom Part of the Soft Robot.

After four hours curing time in ambient environment, demolding procedure starts. In this step, air channel mold is released from the bottom mold. Due to the adhesive forces provided by silicone rubber, demolding procedure requires high-forces to release the air cavity mold. Demolded part is the bottom side of the actuator and it is shown in Figure 4.7.

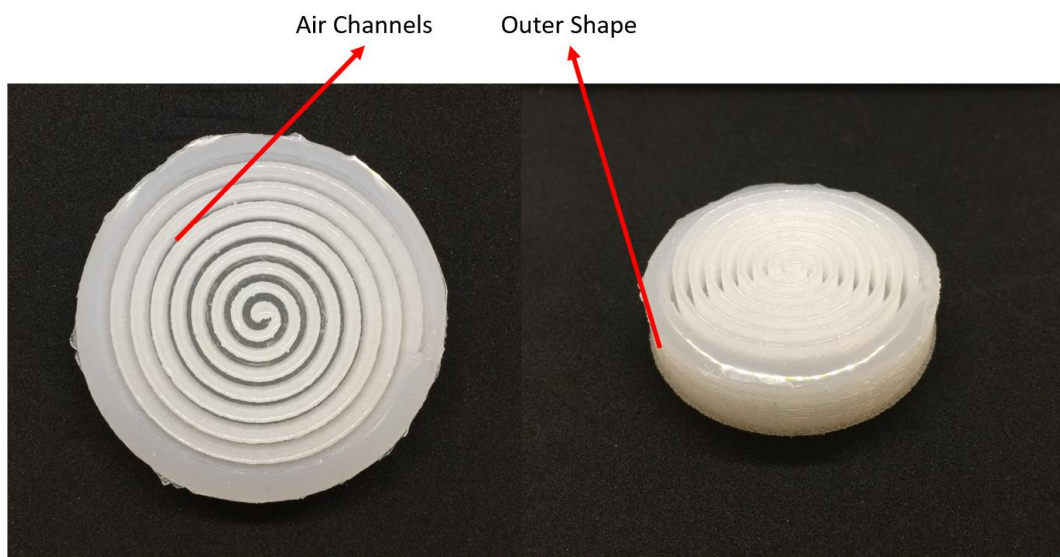


**Figure 4. 7 :** Demolded Silicone, Bottom Side of the Spiral Design.

In order to close the top cover of the actuator, demolded part is placed onto the top cover mold, which is filled with liquid silicone as shown in Figure 4.8. The main reason of assembling the two parts with one in solid form and the other is liquid form is to create perfect sealing to prevent air leakage.

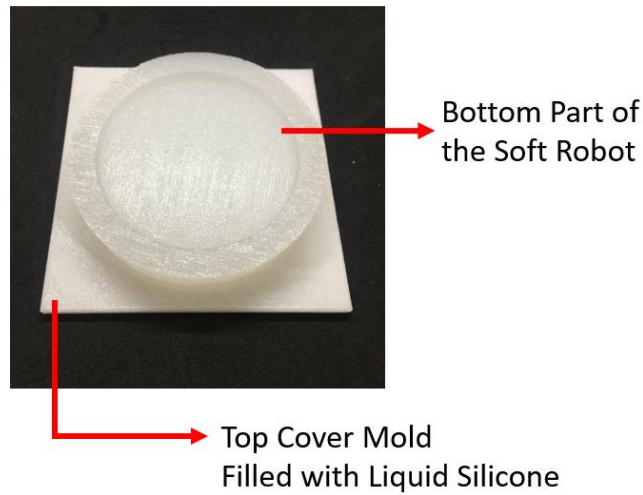


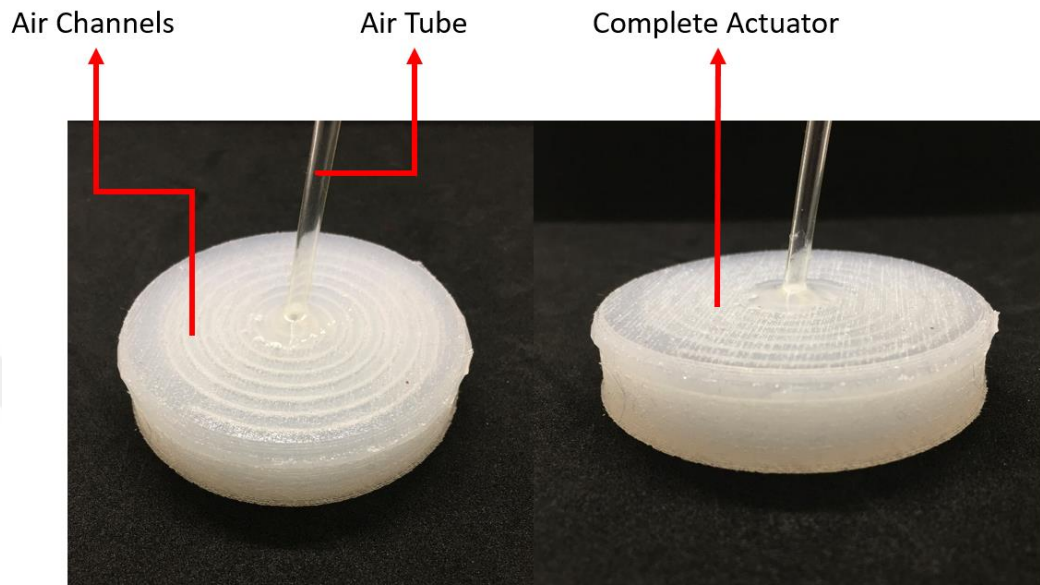
**Figure 4. 8 :** Top Cover Molding.

When the curing procedure is done in four-hour. Completed actuator is demolded from the top cover mold, which will give the result and closed top surface the soft actuator. Thickness of 0.1 mm paper (strain limiting layer) is assembled to the actuator as shown in Figure 4.9.



**Figure 4. 9 :** Strain Limiting Layer Assembly.

Moreover, a tube with 3 mm (inner-diameter) is inserted at the top-center surface of the soft robot to inflate the air channels and the tube is sealed with the same material (Ecoflex 00-30) to the top surface. The complete spiral design of soft actuator is shown in Figure 4.10.

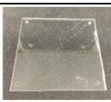


**Figure 4. 10 :** Final Manufactured Soft Robot.

Overall, complete actuator is manufactured with four 3D printed plastic molds, 32 gram Ecoflex 0030 (Smooth-On Inc.), 26 gram for base body and 6 gram for top cover to close the top surface of the actuator, 0.1 mm paper layer, and air tubing to inflate the soft robot.

## 4.2 Experimental Set Ups

Apart from the tools used in manufacturing section, here the experimental study will be explained with the details of equipments, specifications of the components, and schematic view of experimental set-up. First of all bill of materials (BOM) used in the experimental study is shown in Figure 4.11.

Equipment	Name	Where it is used	Count
	Arduino Uno	Micro Controller	1
	3V Micro Air Pump (Max. 40 kPa)	Pressurized Air Supply	1
	L293D, Dual H-Bridge Motor Driver	Air Pump Controlling	1
	Breadboard	Component Connection	1
	Manometer 0-60 kPa	Pressure Measurement	1
	Silicone Tube Ø4 mm (Outer)	Air Inflation	-
	Jumper Cables	Wiring	-
	1/4 Female Fitting	Connection to Manometer	1
	4 mm T Joint	Pipe Joint	1
	Plate with Holes on Corners (40 gr)	Attachment surface	1
	Mass (410 gr)	Suction Force Measurement	1

**Figure 4. 11 : Bill of Materials (BOM).**

The Arduino Uno standard controller board is used which consist of digital input/output pins and ATmega328 micro controller is embedded on the board. Due to the availability in the market Arduino Uno standard board is selected. Next, 3V micro air pump is selected to inflate the actuator, pump has a maximum of 40-kPa air supply, rated voltage is DC 3V, and rated current 460 mA. To control the compressor L293D dual H-bridge motor driver is used. Breadboard and jumper cables are used to connect and assemble the components each other. A manometer is used with the range of 0-60 kPa, to measure the air pressure, which is inserted to the actuator via 4 mm T-joint. ¼ female fitting is used to connect to the manometer in which the other side is fitted to

the air tube and T-joint. Accuracy class of the manometer is KL 1.6, which indicates the full-scale percentage of  $\pm 1.6$ , which gives the  $\pm 0.96$  kPa error. Lastly, acrylic plate (10\*10 cm, 40 gr) is used to place the actuator on it and mass (410 gr) is used to prove the suction force performance of the actuator. In total aim is to create a 450 gram mass to lift by soft robotic actuator. Experimental set-up and schematic connection of the components is presented in Figure 4.12.

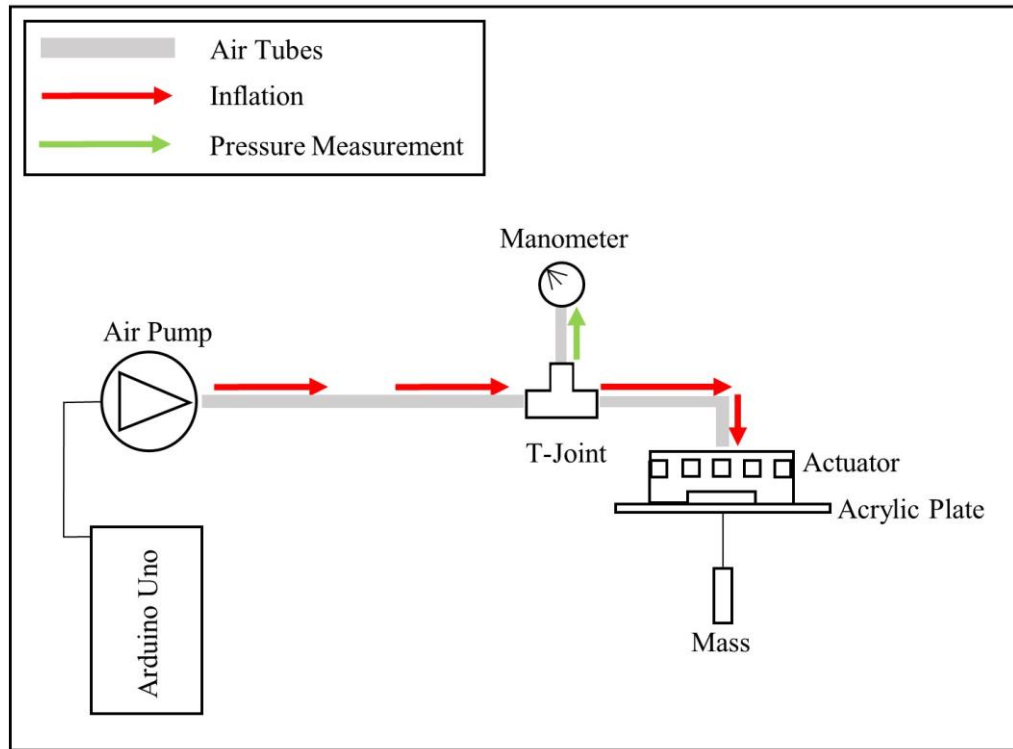


**Figure 4. 12 :** Schematic Representation of Experimental Set-Up.

Detailed three stages in the experimental set-up are presented in Figure 4.12, namely inflation, pressure and suction force measurement. Compressor provides pressurized air to the actuator as it is seen in the Figure 4.12 and with the help of a manometer, which is connected to T-joint, pressure sent to the actuator is measured. When the inflation is done with the desired pressure inside the actuator, compressor is stopped and mass is lifted to prove the vacuum and suction force under the actuator cavity. A more detailed set-up with the real component set-up is shown in Figure 4.13.

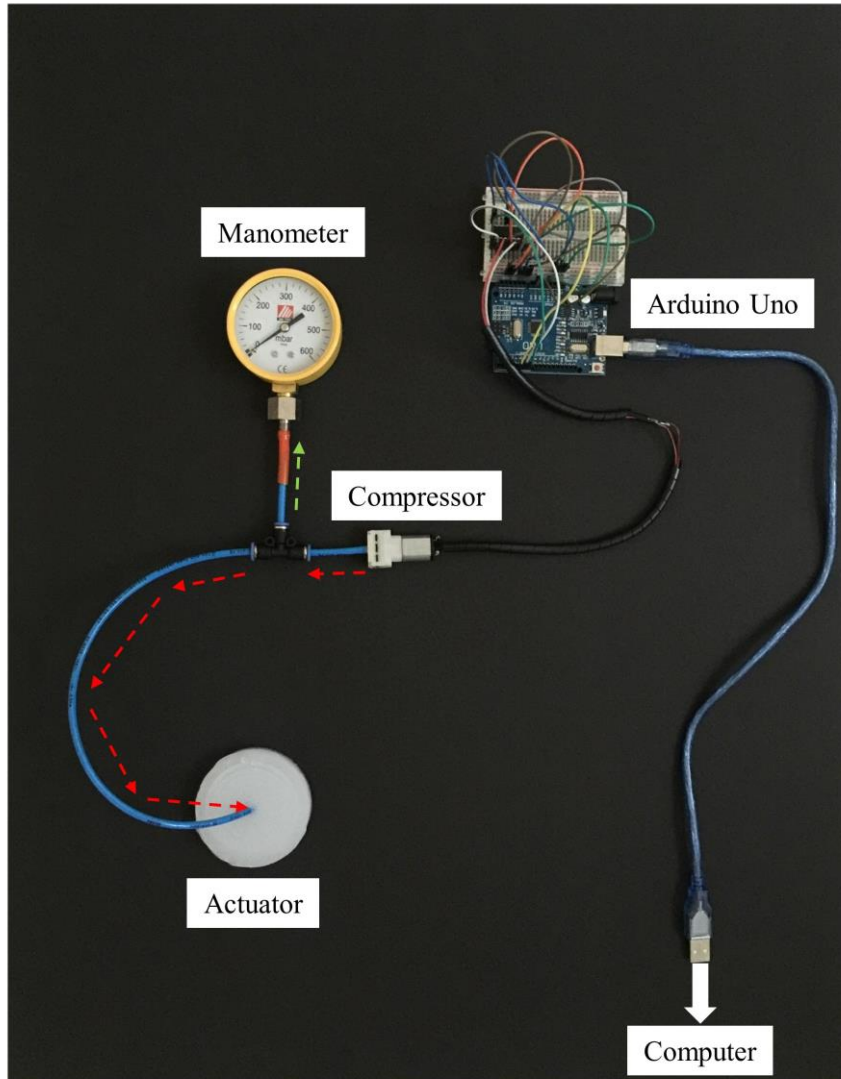


**Figure 4. 13 :** Detailed Experimental Set-up.

### **4.3 Control and Testing**

In this section experimental study's operational conditions and procedure will be explained step by step with the boundary conditions. As it is explained before compressor control is done with the help of motor driver L293D (Texas Instruments) and Arduino Uno. The maximum applicable pressure to the actuator is found 13 kPa with preliminary FEA models. So, in the beginning aim is to find the time-period needed to create desired pressure (13 kPa) inside the actuator's air cavity. Hence, air is supplied to the actuator and pressure is measured with the manometer, when the desired pressure (13 kPa) is read from the manometer, compressor is stopped and the time period is explicitly wrote in the script of Arduino code, which in this case 25000

ms (25 s) and it is written in line-13 in the code block as shown in Figure 4.14. Then, all the experimental study is done based on the actuation time (25 s) which is found explicitly. Complete Arduino script, which explains the compressor control, is given in Figure 4.14.

```

1 int Motor_Pin1 = 6; // pin 2 on L293D
2 int Motor_Pin2 = 5; // pin 7 on L293D
3 int Enable = 7; // pin 1 on L293D
4
5 void setup() {
6     pinMode(Motor_Pin1, OUTPUT);
7     pinMode(Motor_Pin2, OUTPUT);
8     pinMode(Enable, OUTPUT);
9     digitalWrite(Enable, HIGH); //Making the enable pin high to run the motor
10 }
11 void loop() {
12     digitalWrite(Motor_Pin2, HIGH);
13     delay(25000); //Desired time-period to create 13 kPa pressure in the actuator
14     digitalWrite(Motor_Pin1, HIGH);
15 }

```

**Figure 4. 14 :** Compressor Control Arduino Script.

First three line explains the pin-outputs from the L293D and output headers of 6 and 5 are connected to the Arduino pins of 2 and 7 respectively. Void setup block provides output to the coresseponding pins. Moreover, schematic connection diagram of the electronic components (compressor, L293D, and Arduino) is given in Figure 4.15.

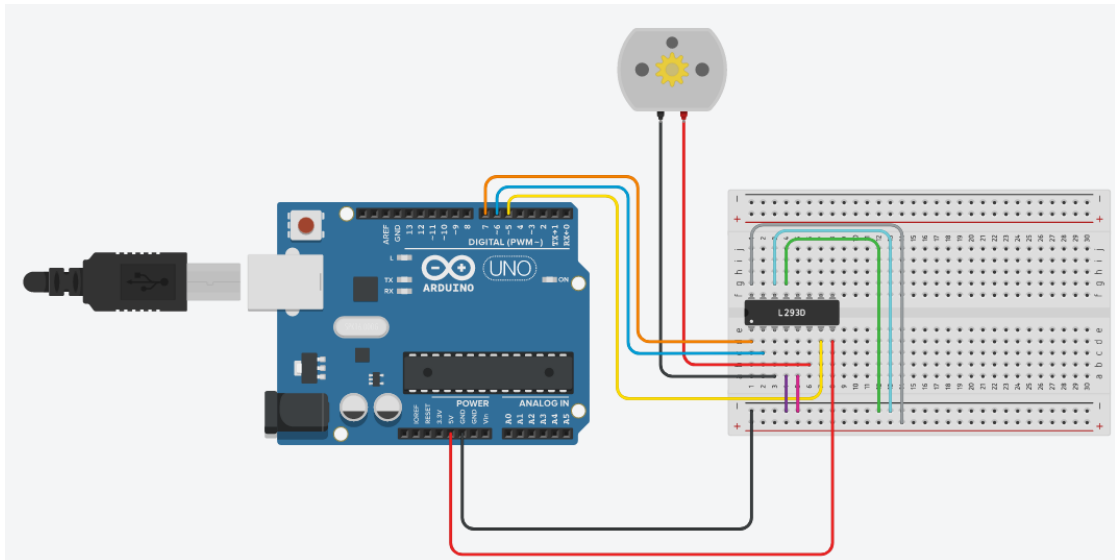


**Figure 4. 15 :** Connection Diagram of the Electronic Components.

To sum up, experimental study of the reference model (spiral design) is pressurized with 13 kPa air, when the desired air pressure is obtained from manometer vacuum pump is stopped (after 25s). Then the actuator tested to lift desired mass.

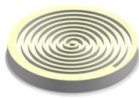
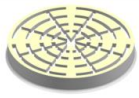
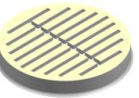


## **5. NUMERICAL STUDY**

In the last years, numerical investigation in the soft robotic field is getting more popular and the reason behind in these phenomena is to understand and predict the behavior of highly elastic materials. Moreover, numerical investigations are used before the manufacturing process in order to do cost reduction and to develop the detailed designs. It is claimed that in the article written by Bell et al. (2018), they had taken the feedback by using finite element simulations with the help of ABAQUS in order to predict the deformations and material behavior. Another example can be given from article written by Qiao et al. (2017), it is stated that they had used to predict suction and spring back effects of hyper-elastic material with the help of ABAQUS finite element simulations. Numerical study of this thesis is performed by ABAQUS standard with non-linear FEA set-up. In this section, finite element model and FEA models will be explained in detail such as unit system, material and contact models, module that is used to predict vacuum and meshing details.

### **5.1 Parametric Finite Element Analysis Study**

In order to differentiate differences between parameters that is being examined, parametric finite element analysis study is conducted. Two main parameters are selected to apply parametric FEA study, paper height and contact area, rest of the parameters mentioned in section three such as air pressure, outer geometry and distances to air cavity from top and bottom surfaces are kept constant for all models. It is decided to use three level value of paper height and contact area and applied to all FEA models. In total forty-five different FEA analysis is done with nine FEA for each design and overview of FEA structure is shown in Figure 5.1.

NAME	SPIRAL	SEMICIRCULAR CHANNEL	CENTER SPIRAL CHANNEL	CIRCULAR CHANNEL	VERTICAL CHANNEL
FIGURE					
NUMBER OF FEA	9 FEA	9 FEA	9 FEA	9 FEA	9 FEA
TOTAL	45 FEA				

**Figure 5. 1 :** Overview of FEA Model Structure.

Differences of FEA models shown briefly in Figure 5.1 are air cavities and the rest of the design parameters are the same such as outer geometry and distances of air cavities to top of the soft robot's surface and bottom.

### 5.1.1 Finite element analysis matrix

In this section, detailed FEA study matrix will be given in order to clarify the model details. As it is mentioned before, paper height and contact area parameters are chosen as three levels. Firstly, the paper height investigations 0,5 mm, 0,3 mm and 0,1 mm height is chosen with the purpose of reflecting the reality and manufacturability, more clearly adding paper layer by layer. Secondly, contact area values are chosen as 586 mm<sup>2</sup>, 950 mm<sup>2</sup> and 1290 mm<sup>2</sup>. Detailed combination of FEA structure for one all models are highlighted in Figure 5.2, with the help of these combinations, every three level of parameters (paper height and contact area) are planned to be examined.

Model Name	FEA Number	Paper Height (mm)	Contact Area (mm <sup>2</sup> )
SPIRAL SEMICIRCULAR CENTER SPIRAL CIRCULAR VERTICAL	1	0,5	586
	2	0,5	950
	3	0,5	1290
	4	0,3	586
	5	0,3	950
	6	0,3	1290
	7	0,1	586
	8	0,1	950
	9	0,1	1290

**Figure 5. 2 :** FEA Model Cases for All Designs.

## 5.2 Finite Element Analysis Model Set Up

In general, every finite element model requires some inputs in order to calculate desired outputs from users. For the cases that require more than one FEA model set up, FEA model template can be used to accelerate the process and reduce the time spend on setting up a model. In this study, it is considered to create one FEA model template that involves same boundary conditions such as material properties, time step settings, boundary conditions and ambient environment conditions for all the forty-five FEA cases mentioned above.

General FEA model set-up includes three main sections such as pre-processing, solver and post-processing starting from CAD design and ending with post-processing the results, details are shown in Figure 5.3.

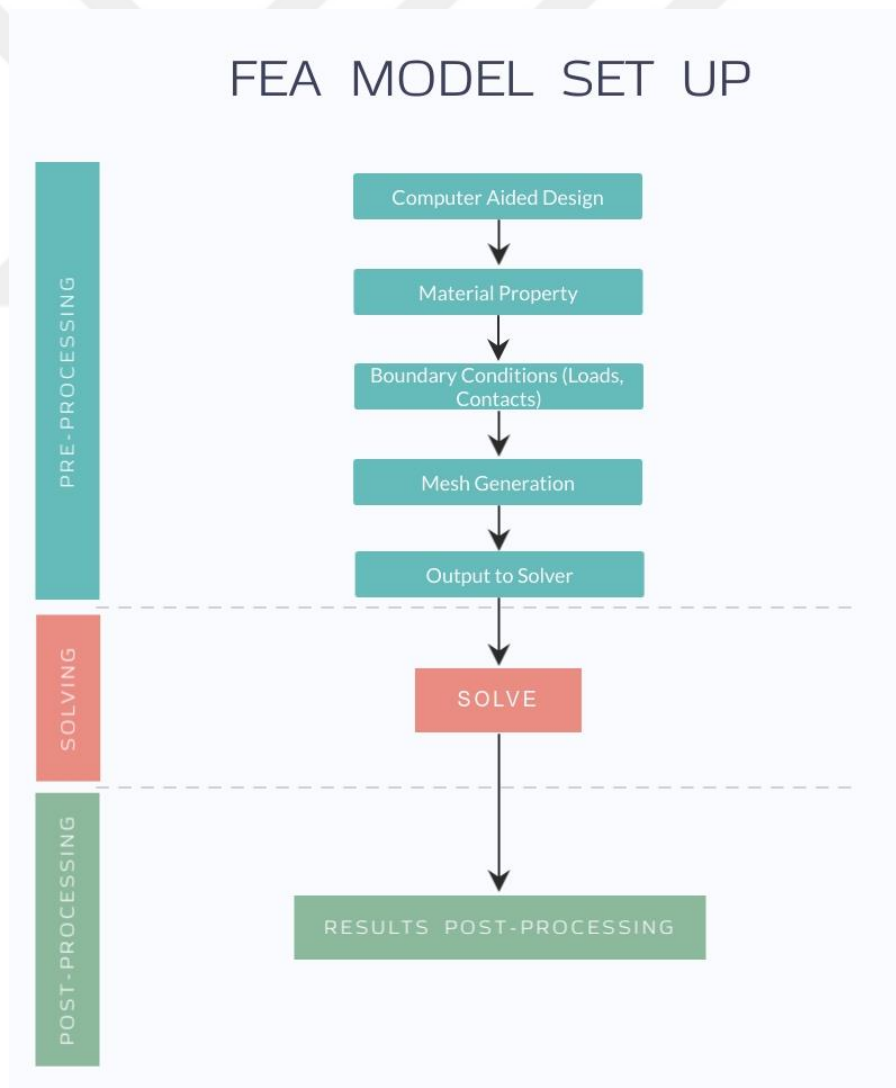


**Figure 5. 3 :** General FEA Model Set-Up.

Diagram above represents the basic finite element analysis steps, procedure starts with computer-aided design, which gives the 3D model of the soft robot, and in this study Siemens NX software is used in order to create 3D models and ABAQUS software is used for finite element analysis procedure. Process continues with defining the material properties to the model, which in this study two material definition is defined in FEA template namely “Ecoflex 00-30” and paper. After that, boundary conditions are defined such as applying pressure to the inner surface of the air cavity, fixed boundary conditions where the soft robot bottom touches to the substrate, paper contact model bottom side of the air cavity surface, point and surface creation for the detection of fluid cavity pressure change where the vacuum will occur. Next, mesh generation, which is the discretization of the 3D model into small parts in order to solve the finite element matrix and boundary conditions. Lastly, when all the model details are proof checked again, input file generated by ABAQUS is ready to transfer to solver. When the model is running in the solver convergence can be checked and monitored inside of the ABAQUS software whether the FEA model is running without any error or not. Final step in FEA model set up is the post-processing the results which is taken out from the solver deck of ABAQUS in the file format of output database (.odb). In this step fluid cavity pressure and volume is checked and the data depends on time is converted into excel file in order to evaluate and compare with the other FEA models.

### **5.2.1 Unit system, ABAQUS**

Every calculation in FEA procedure requires consistent unit system and some FEA software could provide pre set-up unit system but in this study ABAQUS FEA software is chosen and it is a “units-free” software. Being “units-free” system means, that user has to decide the units and set-up the boundary conditions in consistence with each other. In this study, International System of Units (SI) is chosen and all other physical units are derived from force in N and lengths in mm. Consistent unit system used in this thesis is shown in Table 5.1.

**Table 5. 1 : Unit System of FEA in ABAQUS.**

Parameter	Unit (SI)
1. Force	N
2. Length	mm
3. Pressure	MPa (N/mm <sup>2</sup> )
4. Gravity	mm/s <sup>2</sup>
5. Density	tone/mm <sup>3</sup>
6. Absolute Zero Temperature	C°
7. Stefan-Boltzmann Constant	mW/mm <sup>2</sup> *K <sup>4</sup>
8. Universal Gas Constant	mJ/K*mol
9. Ideal Gas Molecular Weight	tone/mol

Unit system and derived other parameters are shown in above Table 5.1. Pressure described in above table represents the pressure applied to the inner side of the air cavity, which makes the soft robot inflatable. Moreover, fluid cavity pressure defined in ABAQUS fluid cavity module and ambient pressure defined in interaction section are derived as MPa. Absolute zero temperature could be chosen in either Kelvin or Celsius, in this case it is chosen as -273.15 C°. Ideal gas molecular weight unit is selected as tone/mol in consisted with density, which based on the same theory Newton and mm.

### 5.2.2 Material models

Material selection criteria of the soft robot is highlighted in a study that is conducted by Hu, Mutlu, Li, and Alici (2018) in terms of availability in the market, manufacturability and accessibility. Moreover, they mentioned that silicone rubber could be molded into different shapes with the help of its liquid form when it is not cured. Another study conducted by Shepherd et al. (2011) is recommended that Ecoflex (Ecoflex 00-30 and Ecoflex 00-50; Smooth-On Inc.) could be used as a base material of soft robot because of it is highly flexible and extensible material structure under low stress. In this study, Ecoflex 00-30 from Smooth-On Inc. is chosen as a base material for soft robot and paper is selected, as inextensible layer because of it is availability and accessibility. For the mathematical modelling side of the hyperelastic non-linear elastomers there are many models can be count for instance Mooney Rivlin, Ogden, Neo-Hooke, Arruda and Boyce. In a study from Abubakar, Myler, and Zhou

(2016) mentioned that elastomers shows a nonlinear elastic behavior and they demonstrate a Cauchy-elastic material form similar to other elastic models, meaning of it explained as stress at each point is obtained with the initial phase of deformation. Moreover, linear elastic and hyperelastic material's stress-strain curves are given in the same study and it is shown in Figure 5.4.

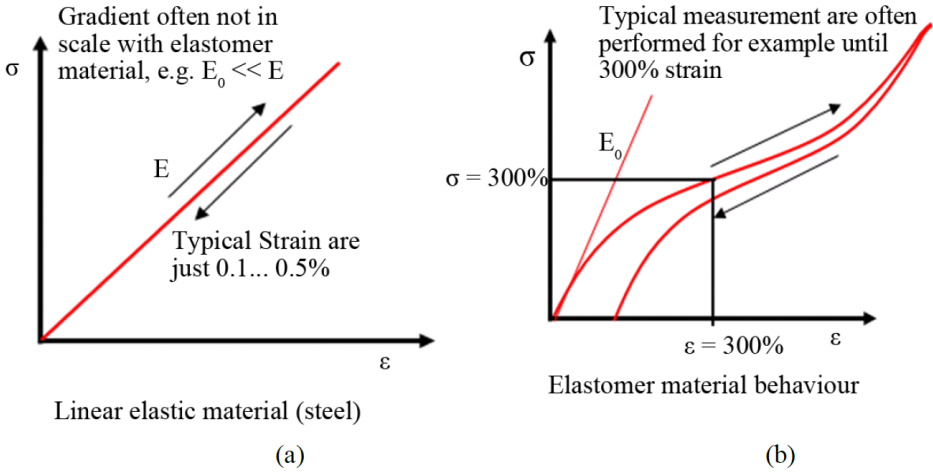


**Figure 5. 4 :** Stress-Strain Curve Comparison, (a) Linear Elastic, (b) Hyperelastic. (Abubakar et al., 2016)

It is mentioned in a study from Yang et al. (2013) the Neo-Hooke material model is mostly used to model rubber-like materials when the material is under linear state and it is said that it does not completely capture material behavior in non-linear and large deformations. However, it is proposed to use Mooney Rivlin material model in order to simulate and predict the non-linear behavior of hyperelastic materials such as Ecoflex 00-30. It is said that in the article Hsu et al. (2013) stress-strain graph of rubber as shown in Figure 5.5, another name hyper-elasticity, could be described by a strain energy density function and it is selected as Mooney Rivlin.

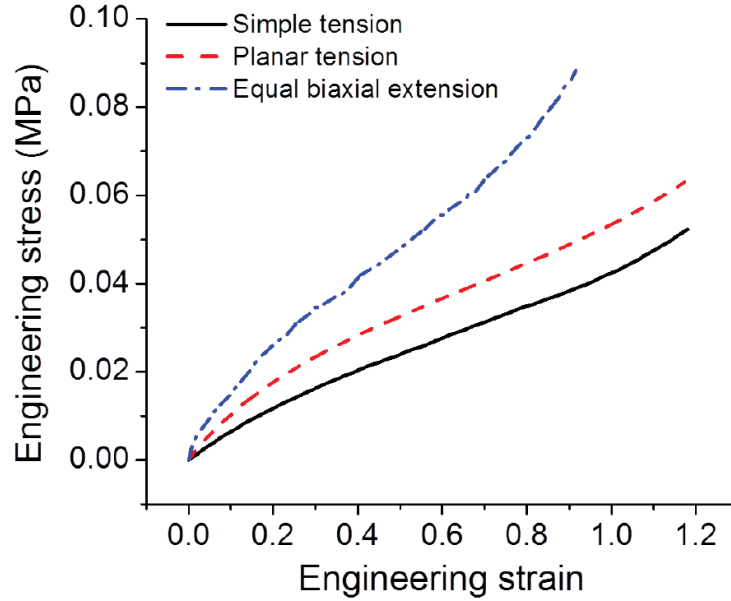


**Figure 5.5 :** Ecoflex 00-30 Stress-Strain Curve. (Hsu et al., 2013)

Additionally, Mooney Rivlin strain energy function is given for incompressible material in below equation 5.1:

$$W = C_{10}(I_1 - 3) + C_{01}(I_2 - 3) \quad (5.1)$$

Where  $W$  stands for strain energy density,  $I_1$  and  $I_2$  describes the first and second strain invariants,  $C_{10}$  and  $C_{01}$  are the material constants calculated as empirically with the equations shown in below equation 5.2 and equation 5.3 (Yang et al., 2013):

$$\mu = 2(C_{10} + C_{01}) \quad (5.2)$$

$$k = \frac{2(C_{10} + C_{01})}{1 - 2\nu} \quad (5.3)$$

Where  $\mu$  is the initial shear modulus,  $\nu$  is the poissons ratio (for an incompressible material almost 0.5 can be assumed) and  $k$  stands for the initial bulk modulus. Material properties for Ecoflex 00-30 are highlighted in the study conducted by Yang et al. (2013) is shown in Table 5.2.

**Table 5.2 :** Material Properties of Ecoflex 00-30. (Yang et al., 2013)

Silicone Rubber	Initial Shear Modulus ( $\mu$ )(MPa)	Initial Bulk Modulus ( $k$ )(MPa)
Ecoflex 00-30	0.009542	0.106017

Material constants that is required to model the FEA material sections are  $C_{10}$  and  $C_{01}$ . They are calculated with the values shown in above Table 5.2 with the equations given in 5.1, 5.2 and 5.3. In addition, same study have obtained the Mooney Rivlin material constants as  $C_{10}$  and  $C_{01}$ , 0.007103 MPa and 0.002332 respectively, and in this study same material constants used in addition with compressibility constant of  $D = 0$  in ABAQUS software. Material constants used in ABAQUS software is shown in Table 5.3 below.

**Table 5.3** : Mooney Rivlin Material Constants, Ecoflex 00-30. (Yang et al., 2013)

$C_{10}$ (MPa)	$C_{01}$ (MPa)	D (Incompressibility)
0.007103	0.002332	0

In addition, paper material properties are given in Table 5.4 below.

**Table 5.4** : Material Properties of Paper. (Yang et al., 2013)

Density (tone/mm <sup>3</sup> )	$E$ (MPa)	$\nu$
8.26	6500	0.2

### 5.2.3 Contact models

Contact models are necessary in FEA for the parts interacting with each other or the part itself. If two independent parts are exist, they will not have any stiffness formulation between each other until any contact formulation is defined. Moreover, stiffness matrix of the problem will be uncoupled and thus one part could be pass through the other part and this might cause an error in the FEA simulation. However, if the proper contact is defined in the problem, contact elements can transmit the contact stress between each other and problem could be solved.

There are mainly two types of contact formulation: first one is “pure penalty method” and second one is “Augmented Lagrangian”. “Pure penalty method” could be explained as setting a spring between two separate parts that have join and touch each other, schematic is shown in Figure 5.6 ("Contact Problem in FEA", 2020).

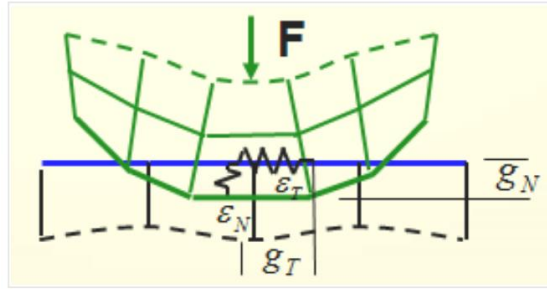


**Figure 5. 6 :** Schematic of Pure Penalty Contact.

Second formulation is Augmented Lagrangian and it can be explained as a derivation of pure penalty method by adding an augmentation to the formulation and aim of this trying the decrease the sensitiveness of contact stiffness.

In this study, in order to model real contact state of paper and soft robot, tie contact is selected due to the manufacturing and assembling of the paper to the soft robot with glue, which is shown in Figure 5.7, paper is highlighted with red rectangle. Tie contact connects two separate surfaces together, which in this case top surface of paper and bottom surface of soft robot, and provides no relative motion among contact pairs.

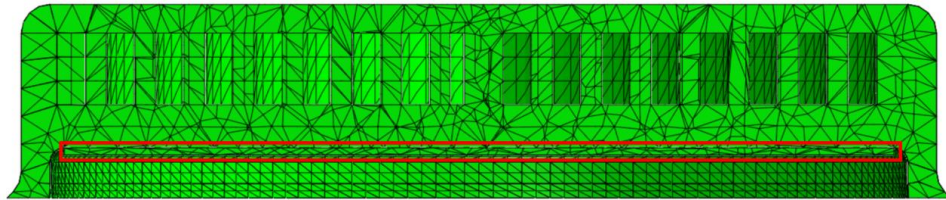


**Figure 5. 7 :** Contact State of the Soft Robot and Paper Layer.

Bottom surface of the actuator is chosen as master surface and top side of the paper is selected as slave surface in ABAQUS tie contact sub-module.

#### 5.2.4 Boundary conditions

In order to simulate the physical effects in FEA boundary conditions are used. It can be said that main boundary conditions in a structural analysis are loading, displacement constraints and thermal effects. In this study there are two main boundary conditions first one is fixed surface of bottom side of soft robot and the second one is pressure load to inner side of the air cavities.

Firstly, fixed boundary condition can be explained with fixing the bottom side of the surface of soft robot where it is touching the substrate. Perfect seal assumption is made

when the touching surface is fixed in FEA model and the surface's translation is constraint with respect to x, y, or z direction. Fixed boundary condition is applied all the forty-five FEA model mentioned in section 5.1.1 and it is shown in Figure 5.8.

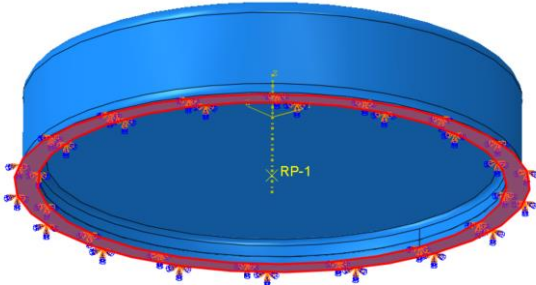


**Figure 5. 8 :** Fixed Boundary condition of Bottom Surface of the Soft Robot.

Secondly, pressure boundary condition can be explained as 13 kPa pressure is applied inner side of the surfaces of the air cavities, the 13 kPa value is found with the help of FEA software in order to apply maximum pressure. It is mentioned in the study conducted by Agarwal et al. (2016) if the actuator FEA results reach a steady state and present stable mechanical behavior after applying pressure into the inner surface of air cavities, airflow dynamics could be neglected. Moreover, only the non-linear static structural FEA model could be used in order to compare the performance of different actuator designs. Similar to Agarwal et al. (2016)'s work, study from Hu et al. (2018) mentioned that pressure boundary condition is applied equally on the inner surface of soft robotic actuator. In this study, same theory from Agarwal et al. (2016) is adopted and performed. Pressure boundary condition and air cavities are shown in Figure 5.9.

	Spiral Design	Semicircular Design	Center Spiral Design	Circular Design	Vertical Design
Applied Pressure in ABAQUS					
Air Cavities					

**Figure 5. 9 :** Pressure Boundary Condition of All Designs.

Figure 5.9 above represents the detailed pressure load that is applied on air cavities, 13-kPa pressure load is applied equally each inner surface of air cavities.

### 5.2.5 Fluid cavity module, ABAQUS

In order to predict the behavior of the soft robot and track the vacuum performance, it is needed to model air under the soft robot vacuum cavity. However, as it is mentioned above, computational fluid dynamics is not used to model fluid-solid interaction; instead fluid cavity module of ABAQUS is used. Fluid cavity module can be used in applications include gas-filled or liquid-filled structures such as pressure vessels, hydraulic or pneumatic mechanisms, airbag simulations. The theory explained in ABAQUS manual and it says reference node is placed inside of the cavity in order to calculate the cavity volume and hence the pressure of it. Theoretical calculation of the volume is shown in Figure 5.10.

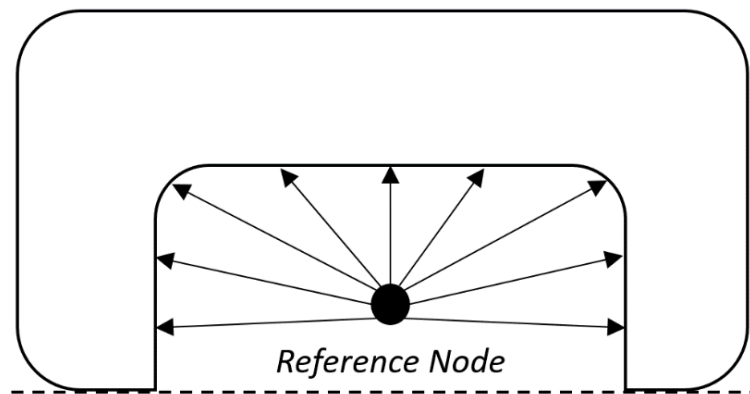


**Figure 5. 10 :** Reference Node and Volume-Pressure Calculation.

Distances to surface of fluid cavity from reference node represents the volumetric surface in Figure 5.10, hence the volume is calculated with this way and based on ideal gas theorem initial pressure is calculated of the cavity. If the volume changes due to the boundary conditions, pressure is determined again iteratively.

The behavior of the fluid model can be hydraulic or a pneumatic model. The pneumatic model is used the theory of ideal gas whereas hydraulic model is based on nearly and fully incompressible fluid behaviors. In this study, pneumatic model is used and air is selected as ideal gas with the molecular weight of  $28,96 \cdot 10^{-6}$  tone/mol and universal gas constant is taken as  $8310 \text{ mJ/K} \cdot \text{mol}$ . Moreover, external ambient pressure of the atmosphere is set in the settings of fluid cavity module, which is taken as  $0.1 \text{ MPa}$ .

First the values are entered in the module section, then the reference node is selected and surfaces that is desired to model the cavity is selected as shown in Figure 5.11.

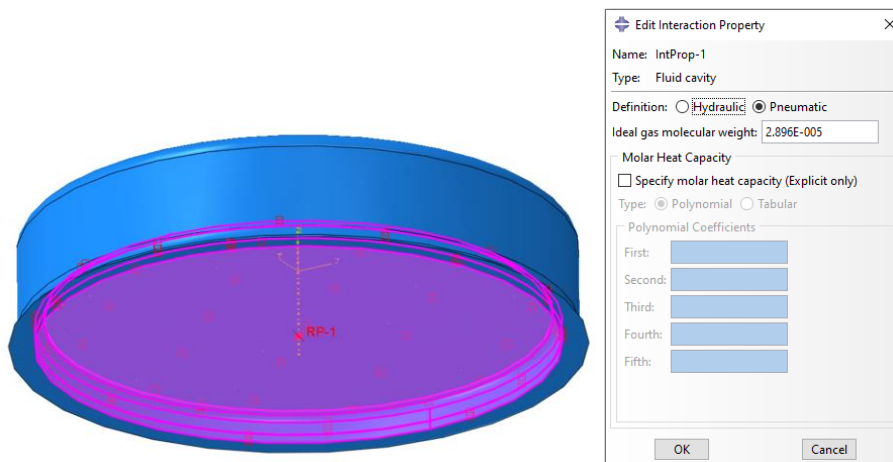


**Figure 5. 11 :** Fluid Cavity Reference Node and Selected Surfaces, a) Selected Surfaces of Fluid Cavity, b) Abaqus Definition of Fluid Cavity.

RP-1 is stands for reference point 1 and the pink surfaces indicates the selected surfaces to model the vacuum cavity of soft robot, blue bottom sides are the surfaces where the soft robot touches the substrate.

### 5.2.6 Mesh model

The precision could be achieved from FEA model is related with the finite element mesh, which represents the 3D model with discretized elements. Subdivided domain is used to solve set of equations in order to simulate physical problem in FEA model. As the elements that represents the problem get smaller, accuracy of the solution is increases until at a point where the solutions not change, this point is called convergence and the procedure is called mesh refinement.

In ABAQUS software there are four meshing techniques could be used namely: free meshing, sweep meshing, structured meshing and bottom up meshing. Mainly there are three element types used in FEA models, which they are 1D, 2D and 3D. Although, there are 1D and 2D element solutions are faster in many cases, in this study free meshing technique is used with 3D elements, which is proper for the 3D model representation. Moreover, non-linear FEA models mostly use 2<sup>nd</sup> order finite element mesh in order to represents the geometry under loading in deformation states. It is also valid for the soft robotic FEA studies where the material non-linearity is valid. In general, for the 3D analysis in ABAQUS there are four different quadratic tetrahedral

element type could be chosen namely C3D10, C3D10M, C3D10H and C3D10I. C3D10H element type is hybrid element and H indicates the hybrid, this element class is intended to represent the incompressible material simulations. Schematic representation of C3D10 element is shown in Figure 5.12 ("Ten-node tetrahedral element (C3D10 and F3D10)", 2020).

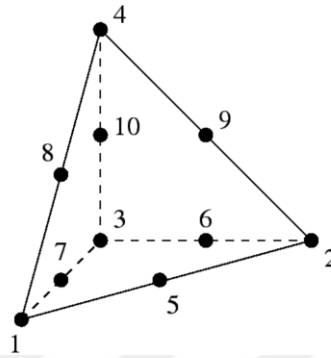
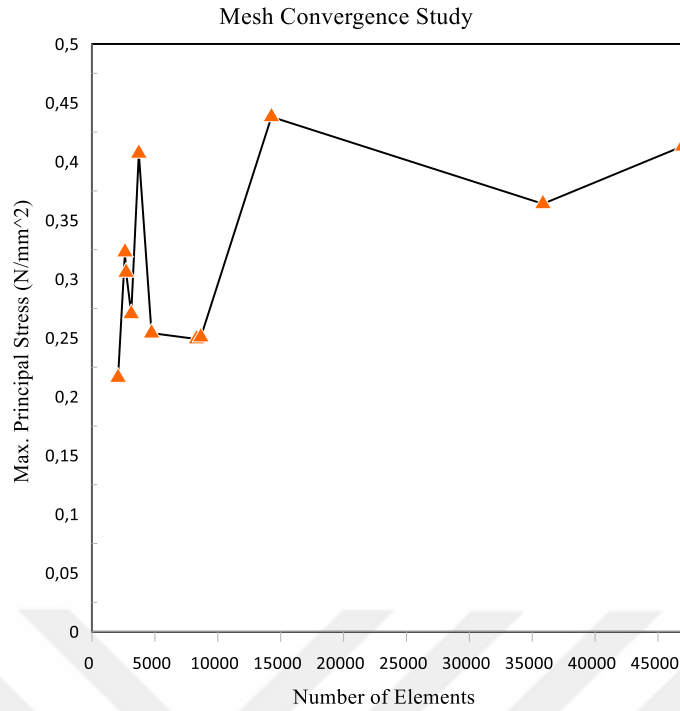


**Figure 5. 12 :** 3D 10-Node Tetrahedral Element, 2<sup>nd</sup> Order.

Similar to C3D10 shown in Figure 5.16, C3D10M, C3D10H and C3D10I has the same schematic representation.

Study conducted by Qiao et al. (2017) mentioned that 2<sup>nd</sup> order 2D quadrilateral CAX4H elements are used in non-linear FEA model. Another study from Z. Wang et al. (2017) used 3D quadratic hybrid elements with 10 node in order to represent the soft robotic actuator.

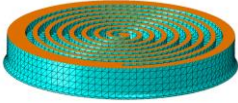
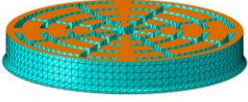
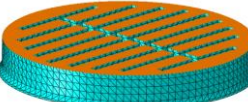
A mesh convergence study is conducted for the spiral design FEA model with the configurations of 1290 mm<sup>2</sup> contact area and it is measured based on the maximum principle stress on the model. It is found that the 2 mm element size with 35852 total number of element model shows convergent mesh independent results, hence it is decided to use 2 mm element size rather than 1.75 mm, to reduce the time for solving the FEA model. Mesh convergence study results are shown in Figure 5.13.



**Figure 5. 13 :** Mesh Convergence Study Results.

In this study 3D tetrahedral 2<sup>nd</sup> order hybrid formulation element is used for the soft robot body discretization. Each soft robotic design has the same element type with different element numbers. Element information and element number for each soft robotic design is highlighted in Table 5.5.

**Table 5. 5 :** Finite Element Mesh Details for Each Design.

Soft Robot Design	Mesh	Element Type	Total Element
Spiral Design		C3D10H	35852
Semicircular Design		C3D10H	29931
Center Spiral Design		C3D10H	36704
Circular Design		C3D10H	37632
Vertical Design		C3D10H	36051

## **6. RESULTS AND DISCUSSION**

In this section, results of experimental and finite element analysis studies will be given and explained over five different soft robotic actuator design. As it was mentioned before there will be forty-five FEA results which consist of vacuum pressure and theoretical suction force calculations, and each design section will be compared first in its design cases and then with other designs.

Firstly, as it is mentioned before in section 4.3, spiral design (with paper layer) experiments are done and results are presented. In the first sub-section, experimental results of the reference model will be given, which is the spiral design, with paper strain limiting layer. Output of the experimental study will be measured air pressure that is sent to the actuator (in kPa) and the experimental load lifting capacity (suction force) of the soft robot (in Newton), which will further validate the vacuum pressure obtained from FEA study and theoretical calculation of suction force.

Secondly, numerical results of the spiral design will be validated with the result of experimental study and correlation of the results will be presented. This procedure will show the accuracy FEA model as well as the percentage of the result error, so the other four unique design FEA models will be used to estimate vacuum performance and suction force.

Third, numerical results of the other four actuator's vacuum pressures that is obtained from the FEA studies and suction forces will be given. Process follows the procedure: first, vacuum pressure values created by soft robotic actuator are obtained from ABAQUS software. Then values are transferred to excel sheet in order to do the unit conversions. Secondly, theoretical suction force calculations will be done based on the formula explained in section 2.2.3 and Figure 2.6. Thus, graphical representation of the comparative study of the FEA results will be given.

Finally, a detailed discussion will be given over forty-five different results obtained from both FEA and experimental study, and results will be explained with reasons.

## 6.1 Experimental Results

In this section all the experimental results of the reference model (spiral design with paper layer) will be given. As it is mentioned in 4.3, actuator is pressurized with 13-kPa air then its suction force capability is tested with 450 g mass lifting. Experimental study set-up of reference model (spiral design) is shown in Figure 6.1 with the details of: beginning of the test, actuation of the soft robotic actuator with 13-kPa air pressure, and lifting the mass of 450g.

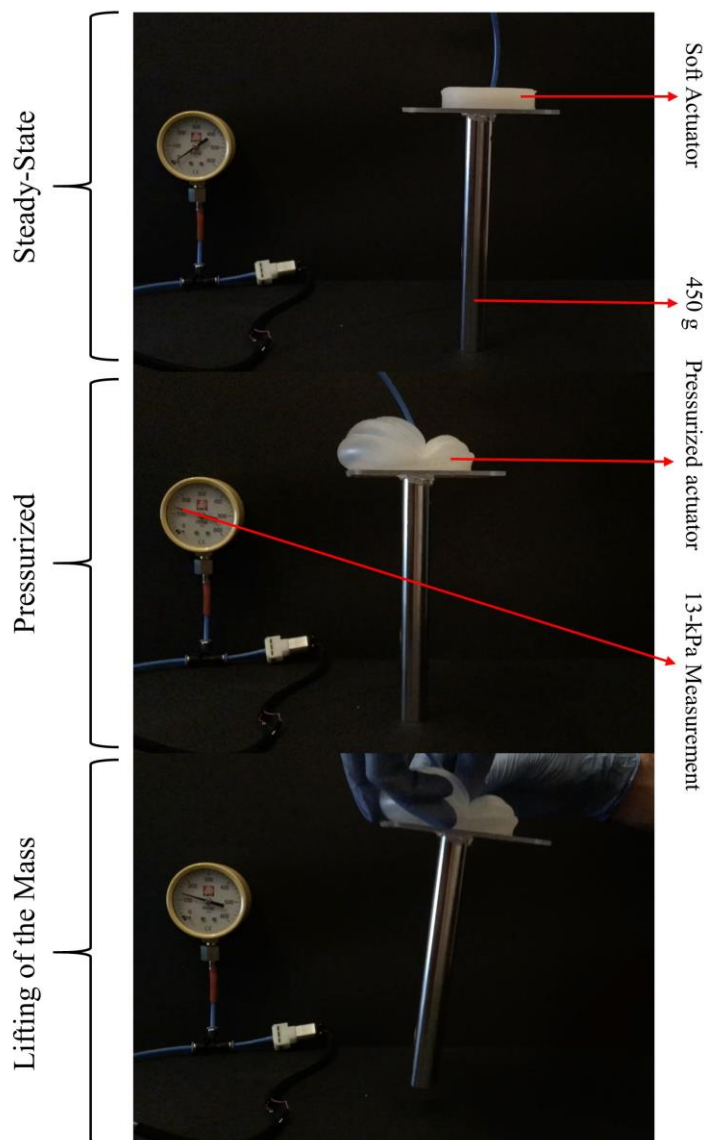


**Figure 6. 1 :** Experimental Study Results of Reference Model (Spiral Design).

As it is shown in Figure 6.1 spiral design of the soft actuator body is found that capable of lifting 450g mass with 13-kPa pressure inside the air cavities.

## 6.2 Finite Elementa Analysis Model Validation

In this section, finite element analysis results of the spiral design (reference model) with 0.1 mm paper layer will be validated with the experimental results. Firstly, as it is mentioned in section 5.2.4, boundary conditions are; 13-kPa pressure applied on the wall of the actuator, 0.1 mm paper layer is applied with tie contact to the soft actuator body, and fixed boundary conditions are applied to the attachment surface of the actuator. Finite element model results and experimental results of the actuator are given in Figure 6.2.

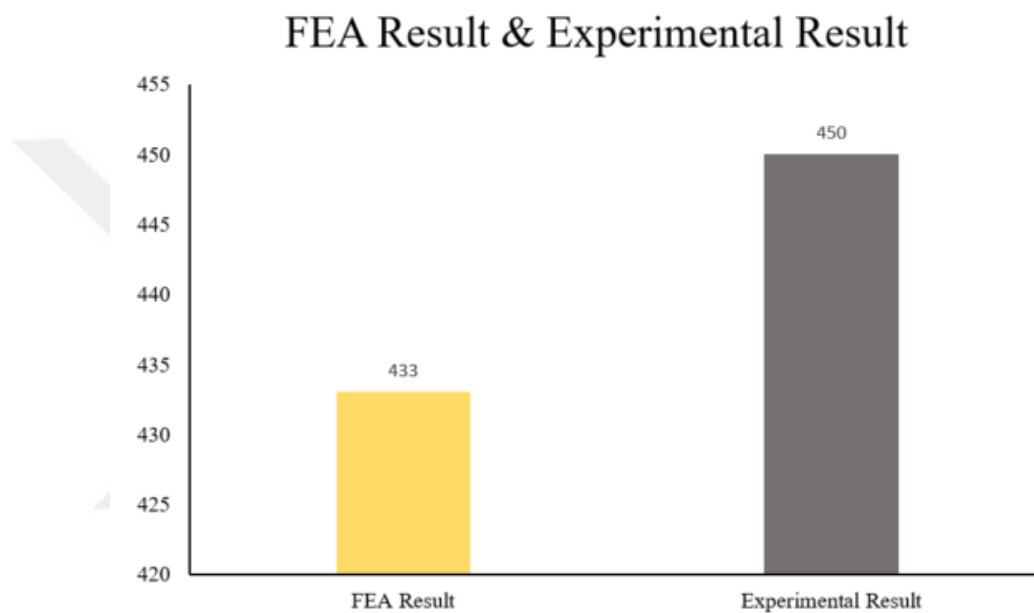


**Figure 6. 2 :** Validation of the FEA Model with Experimental Results.

As it is shown above, according to the experimental results, actuator is capable of 450g mass and according to the simulation results, it is capable of lifting 433g (4.25 N) mass. Approximate error between the experimental and FEA result is calculated as % 3.8.

## 6.3 Finite Element Analysis Results

In this section, complete finite element analysis study results will be given over five actuator designs.

Firstly, spiral design soft robotic actuator FEA results will be presented such as vacuum pressure in kPa and suction force in Newton. Results will be represented in a matrix table as shown in Figure 6.3 which shows the nine different case studies include

paper height levels (0,5 mm - 0,3 mm - 0,1 mm) and contact area levels (586 mm<sup>2</sup> - 950 mm<sup>2</sup> - 1290 mm<sup>2</sup>).

VACUUM PRESSURE (kPa)				
SPIRAL DESIGN		Contact Area		
		586	950	1290
Paper Height	0,5	2,34	2,95	3,21
	0,3	2,52	3,04	3,24
	0,1	2,71	3,12	3,29

a)

SUCTION FORCE (N)				
SPIRAL DESIGN		Contact Area		
		586	950	1290
Paper Height	0,5	1,37	2,8	4,15
	0,3	1,47	2,89	4,18
	0,1	1,59	2,96	4,25

b)

**Figure 6. 3 :** Spiral Design FEA Results, a) Vacuum Pressure, b) Suction Force.

In addition to the vacuum pressures and suction forces given in Figure 6.3, more detailed representation of vacuum pressure-FEA cases graph is shown in Figure 6.4. Highest vacuum pressure obtained from the design cases is shown with case number-9 in which the parameter combination of contact area 1290 mm<sup>2</sup> with paper height 0,1 mm.

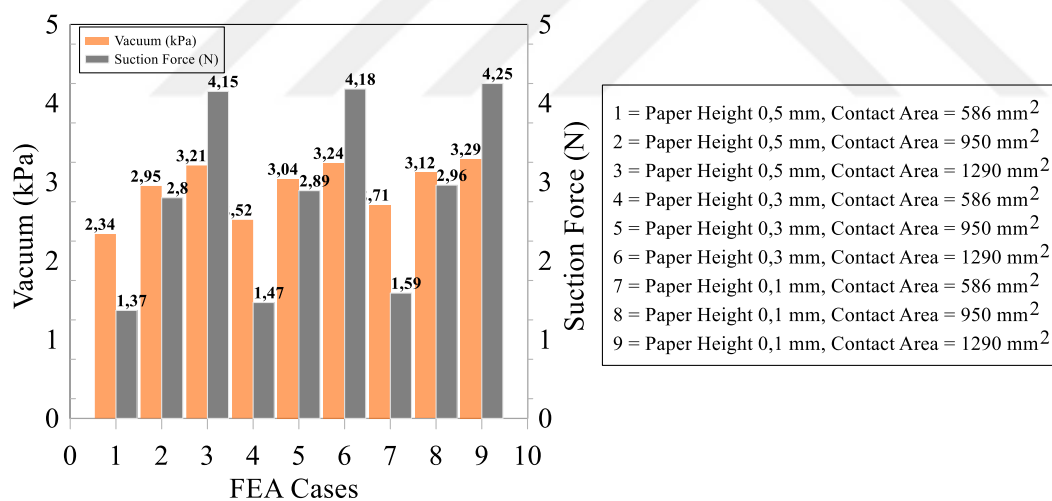


**Figure 6. 4 :** Vacuum Pressure Graph (Spiral Design).

Finite element analysis result of the spiral design is given in Figure 6.5 with the maximum displacement results of 9.33 mm. Red color location is the area where the spiral end of the air channel nearest to the outer wall of the actuator.

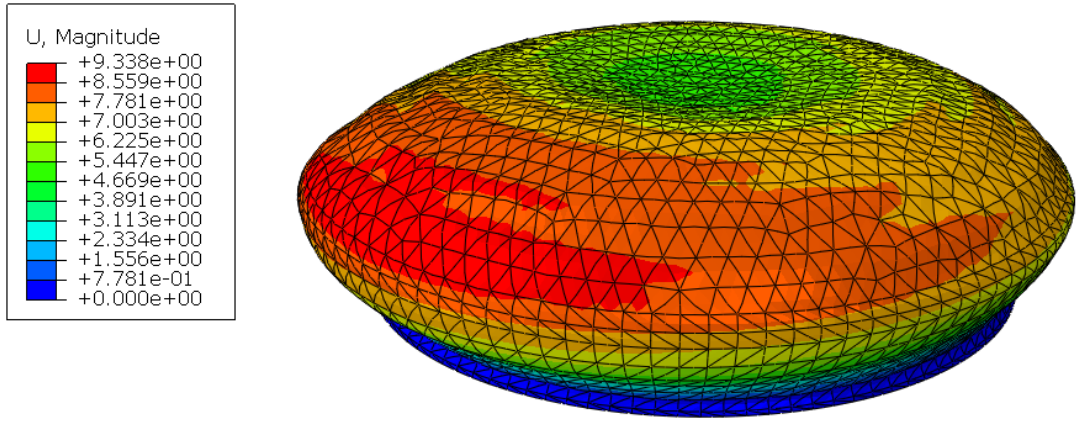


**Figure 6. 5 :** Displacement Result of Spiral Design.

Secondly, semicircular design of soft robotic actuator vacuum pressure and suction force FEA results matrix are given in Figure 6.6, and detailed vacuum pressure-FEA cases graph is demonstrated in Figure 6.7 respectively.

		VACUUM PRESSURE (kPa)					SUCTION FORCE (N)		
		SEMICIRCULAR DESIGN					SEMICIRCULAR DESIGN		
		Contact Area					Contact Area		
		586	950	1290			586	950	1290
Paper Height	0,5	2,98	3,88	4,14	Paper Height	0,5	1,74	3,68	5,34
	0,3	3,22	4,04	4,31		0,3	1,88	3,84	5,56
	0,1	3,29	4,22	4,49		0,1	1,93	4,01	5,79

**Figure 6. 6 :** Semicircular Design FEA Results, a) Vacuum Pressure, b) Suction Force.

The highest vacuum pressure and suction force achieved from the model is given with case number 9, in which the vacuum pressure is calculated as 4.49 kPa and suction force value as 5.79 N. General trend can be seen in Figure 6.7, vacuum and suction force values are increased with an increase in the contact area and decrease in paper height level.

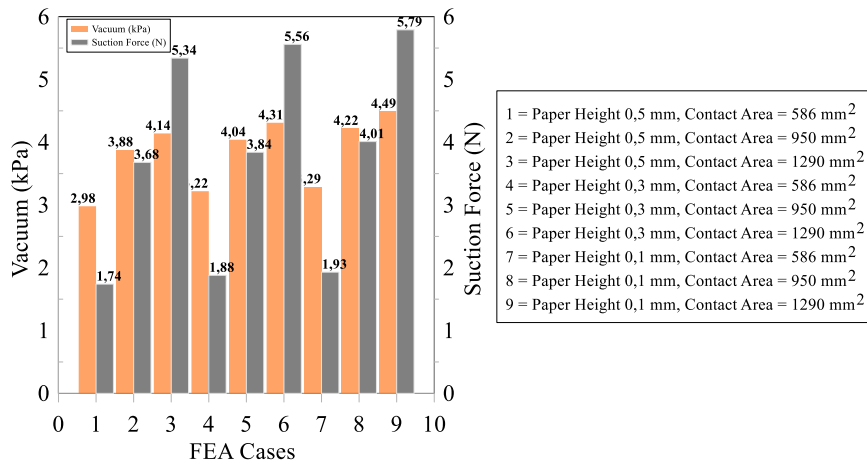


**Figure 6. 7 : Vacuum Pressure Graph (Semicircular Design).**

Displacement result of the semicircular design is given in Figure 6.8 with the maximum of 19.8 mm. The most deformed area is the place where the material is not in contact with bottom surface of the actuator. Hence, the partial inflation of the outer shape is related to the material overbuild in these locations.

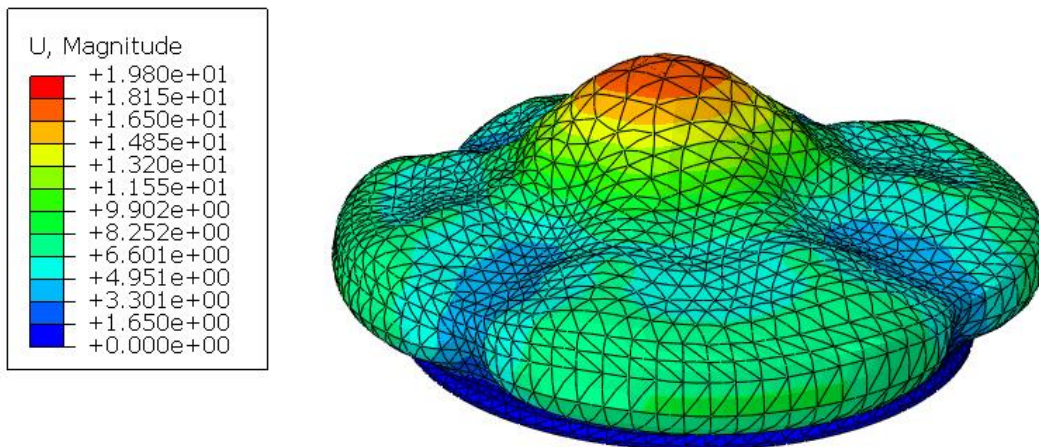


**Figure 6. 8 : Displacement Result of Semicircular Design.**

Thirdly, FEA matrix of Central Spiral design are given below in Figure 6.9 and vacuum pressure-FEA cases graph in Figure 6.10 respectively. As it is seen in the results vacuum pressure is obtained from the model is 4.84 N and suction force is 6.25 N with the combination of 1290 mm<sup>2</sup> contact area and 0.1 mm paper height.

VACUUM PRESSURE (kPa)				
CENTER SPIRAL DESIGN		Contact Area		
		586	950	1290
Paper Height	0,5	2,66	3,6	4,35
	0,3	3,01	3,81	4,55
	0,1	3,48	4,18	4,84

a)

SUCTION FORCE (N)				
CENTER SPIRAL DESIGN		Contact Area		
		586	950	1290
Paper Height	0,5	1,56	3,42	5,61
	0,3	1,76	3,62	5,87
	0,1	2,03	3,97	6,25

b)

**Figure 6. 9 :** Center Spiral Design FEA Results, a) Vacuum Pressure, b) Suction Force.

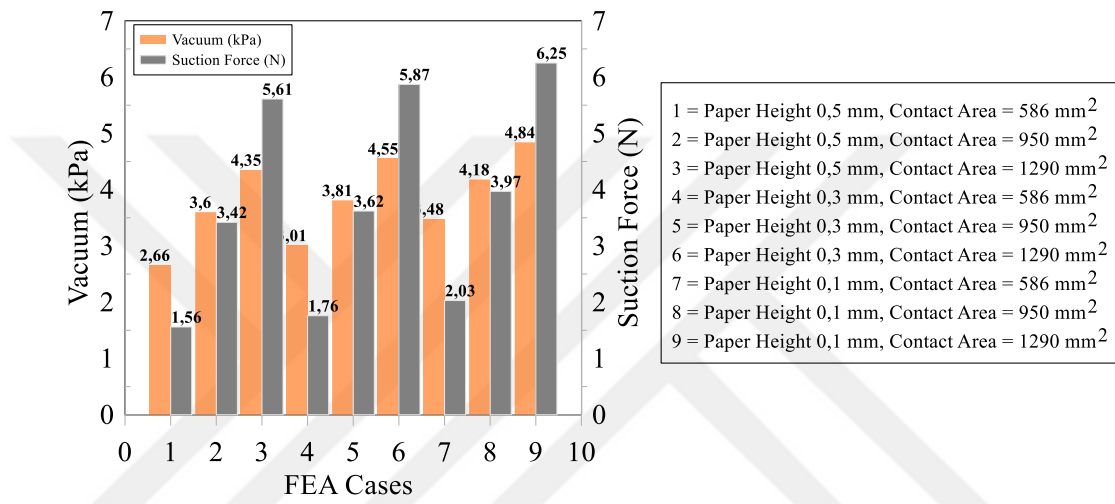


**Figure 6. 10 :** Vacuum Pressure Graph (Center Spiral Design).

In addition, simulation result of the center spiral design is given in Figure 6.11 with the value of displacements at the left hand side. The maximum suction force and the maximum displacement is found to be in correlation, and the maximum displacement of the center spiral design is 30.56 mm.

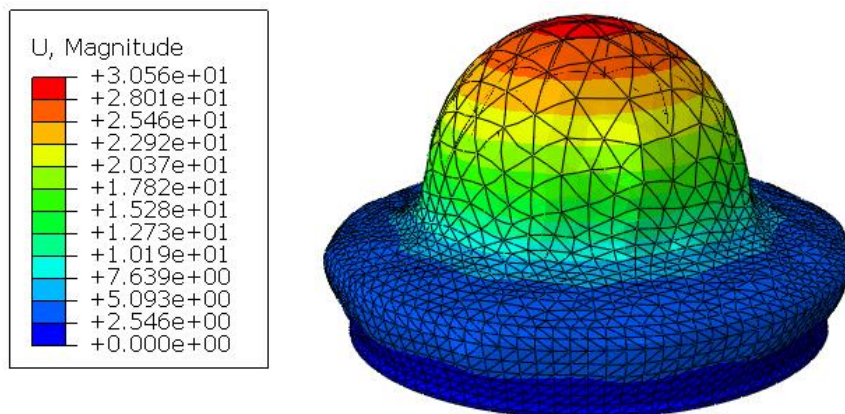


**Figure 6. 11 :** Displacement Result of Center Spiral Design.

Next, circular design results are shown below in Figure 6.12 and vacuum pressure-FEA cases graph in Figure 6.13. The maximum vacuum pressure and suction force obtained from the circular design is 1.56 kPa and 2.01 N respectively.

CIRCULAR DESIGN		VACUUM PRESSURE (kPa)		
		Contact Area		
Paper Height	0,5	0,86	1,17	1,4
	0,3	0,98	1,28	1,48
	0,1	1,09	1,37	1,56

a)

CIRCULAR DESIGN		SUCTION FORCE (N)		
		Contact Area		
Paper Height	0,5	0,5	1,11	1,81
	0,3	0,57	1,21	1,92
	0,1	0,64	1,3	2,01

b)

**Figure 6. 12 :** Circular Design FEA Results, a) Vacuum Pressure, b) Suction Force.

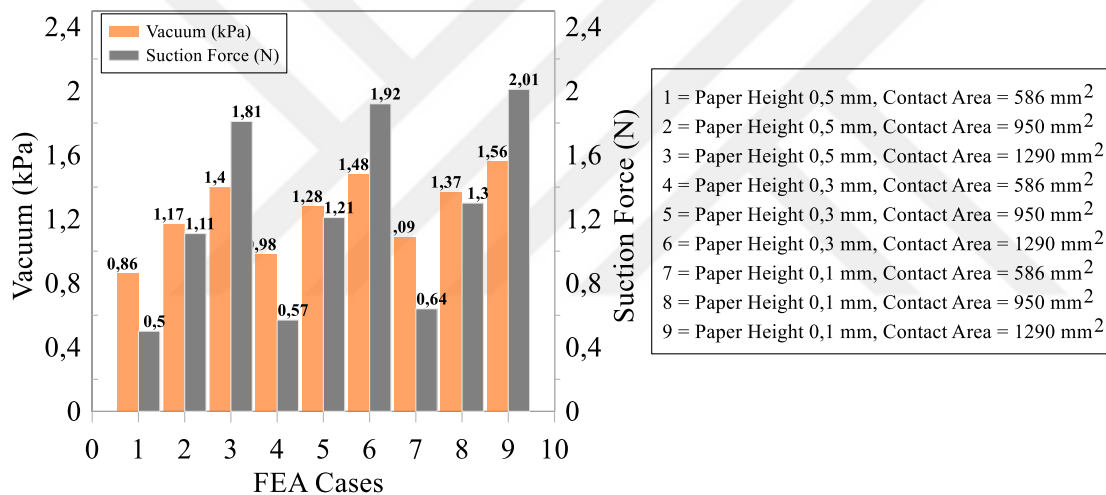


**Figure 6. 13 :** Vacuum Pressure Graph (Circular Design).

Finite element simulation results of the circular design is given in Figure 6.14 with the maximum displacement of 12.29 mm. It is found that the circular design is the third actuator with minimal displacement after the spiral design.

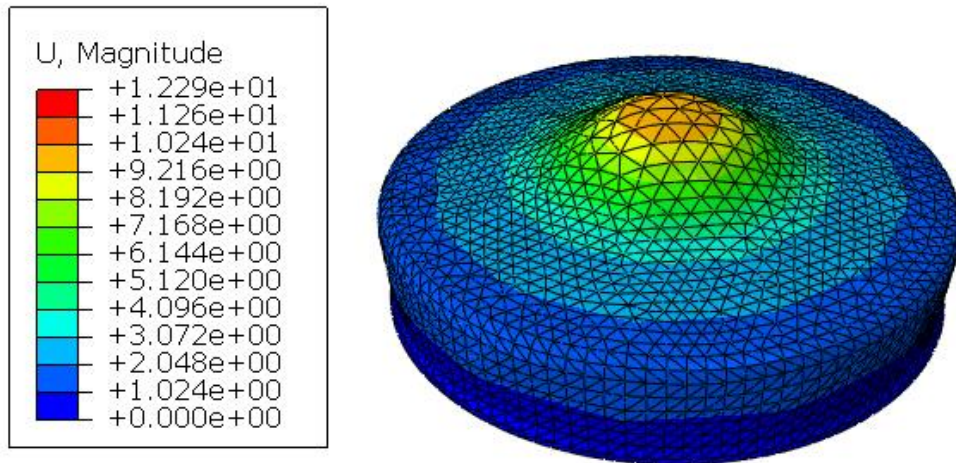


**Figure 6.14 :** Displacement Result of Circular Design.

Finally, result matrix of vacuum pressure and suction force of vertical design are given in Figure 6.15 and vacuum pressure-FEA cases graph is shown in Figure 6.16 with the maximum suction force of 3.05 N and the vacuum pressure of 2.36 kPa respectively.

VACUUM PRESSURE (kPa)				
VERTICAL DESIGN		Contact Area		
		586	950	1290
Paper Height	0,5	1,46	1,86	2,14
	0,3	1,6	1,99	2,26
	0,1	1,76	2,11	2,36

a)

SUCTION FORCE (N)				
VERTICAL DESIGN		Contact Area		
		586	950	1290
Paper Height	0,5	0,85	1,77	2,76
	0,3	0,93	1,89	2,92
	0,1	1,03	2,01	3,05

b)

**Figure 6.15 :** Vertical Design FEA Results, a) Vacuum Pressure, b) Suction Force.

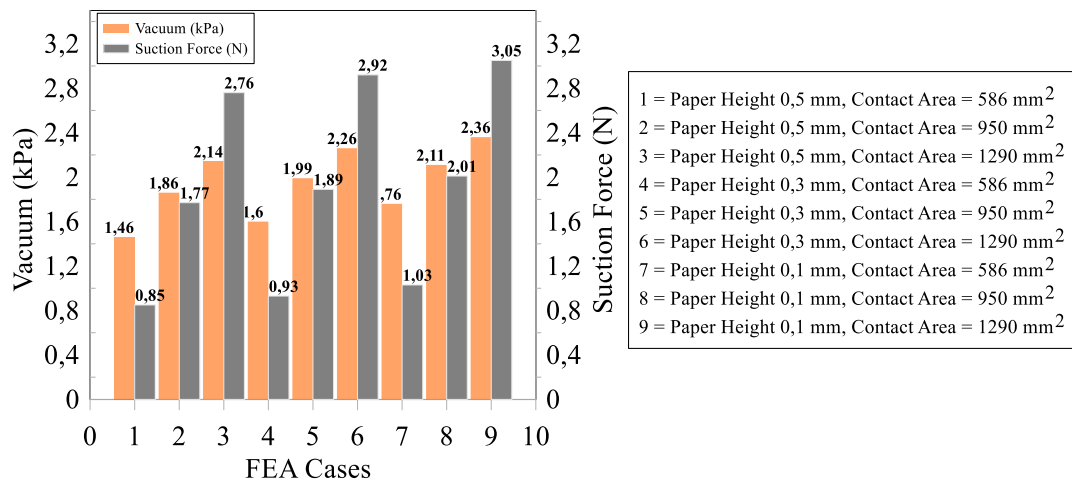


**Figure 6.16 :** Vacuum Pressure Graph (Vertical Design).

Finally, vertical design displacement results are given in Figure 6.17 with the value of 7.86 mm and it is found that the vertical design is the actuator has minimal displacement among all actuators.

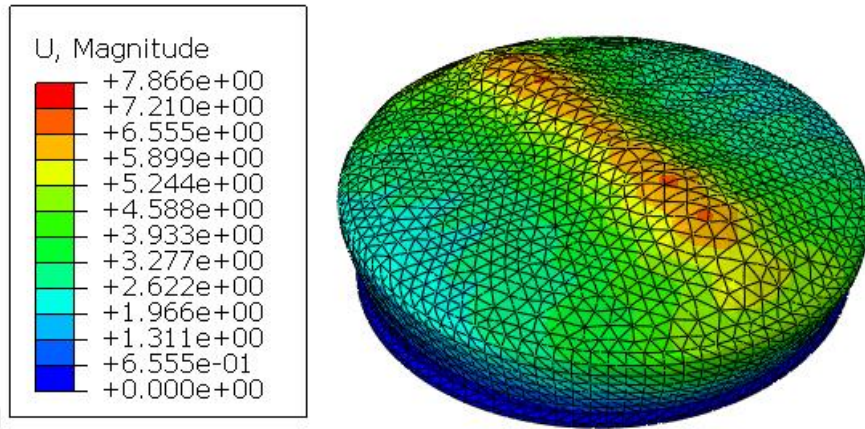


**Figure 6.17 :** Displacement Result of Vertical Design.

All the forty-five FEA results of vacuum pressure and suction forces over five actuator designs are given above in Figures 6.3-17. To better understand the resulting pattern in the FEA cases, comparative graphical representation will be given which is depended on parameters such as contact area and paper height. Firstly, relation of the contact area and vacuum pressure will be shown, and then contact area and suction force will be given. Secondly, paper height and vacuum pressure as well as suction force relation will be demonstrated.

Vacuum pressure (kPa) variation with the contact area (586, 950 and 1290 mm<sup>2</sup>) is shown in Figure 6.18, based on the paper heights 0,1, 0,3 and 0,5 mm respectively.

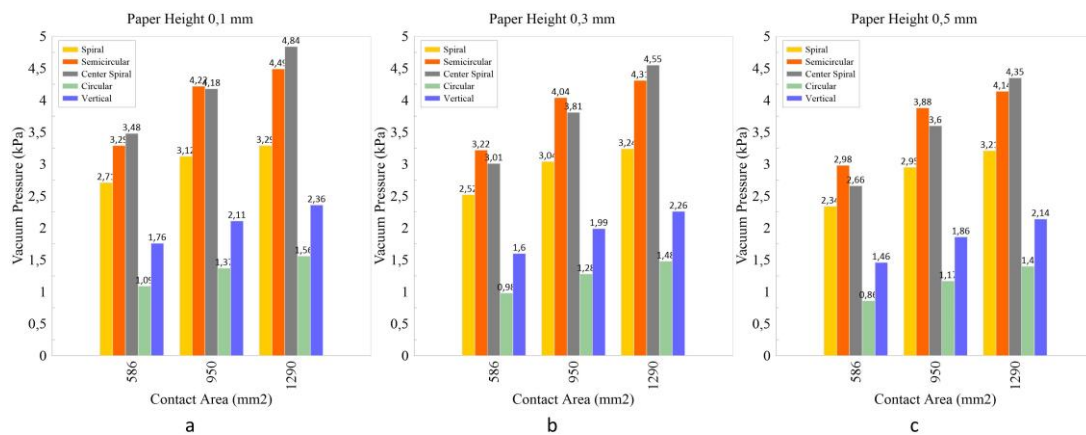


**Figure 6.18 :** Contact Area and Vacuum Pressure, for Paper Heights: a) 0,1 mm, b) 0,3 mm, c) 0,5 mm.

It can be seen that, in spiral design with 0.1, 0.3, and 0.5 mm paper heights, when the contact area increased from 586 mm<sup>2</sup> to 950 mm<sup>2</sup> and 1290 mm<sup>2</sup>, general trend shows that vacuum pressure is increased in all design cases. However, the maximum vacuum pressure is obtained from the design cases is the center spiral design with 0.1 mm paper height level and 1290 mm<sup>2</sup> contact area, and the pressure is 4.84 kPa.

In addition to the vacuum pressure, another output is the suction force and its relation with the contact area demonstrated below in Figure 6.19. The calculation procedure of the suction force is given in section 3.2.2 with the formula of 3.3.

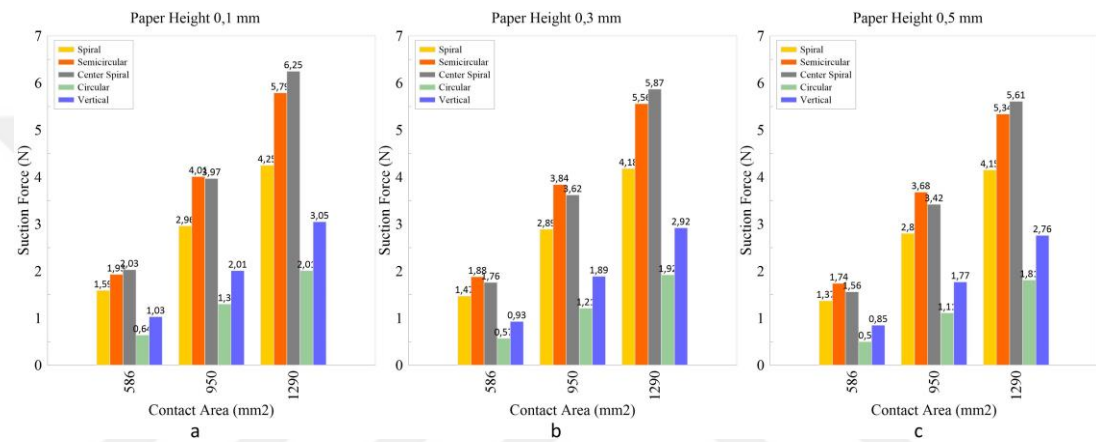


**Figure 6. 19 :** Contact Area and Suction Force, for Paper Heights: a) 0,1 mm, b) 0,3 mm, c) 0,5 mm.

Based on the results and calculation formula, it is clearly seen from the bar charts, suction force is increased when the contact area is increased in all design cases. Moreover, the maximum suction force is obtained from the actuator designs is 6.25 N, which belongs to center spiral design with 0.1 mm paper height layer.

Same comparative study for the paper heights and vacuum pressure as well as suction force is presented below in Figure 6.20 and 6.21 respectively.

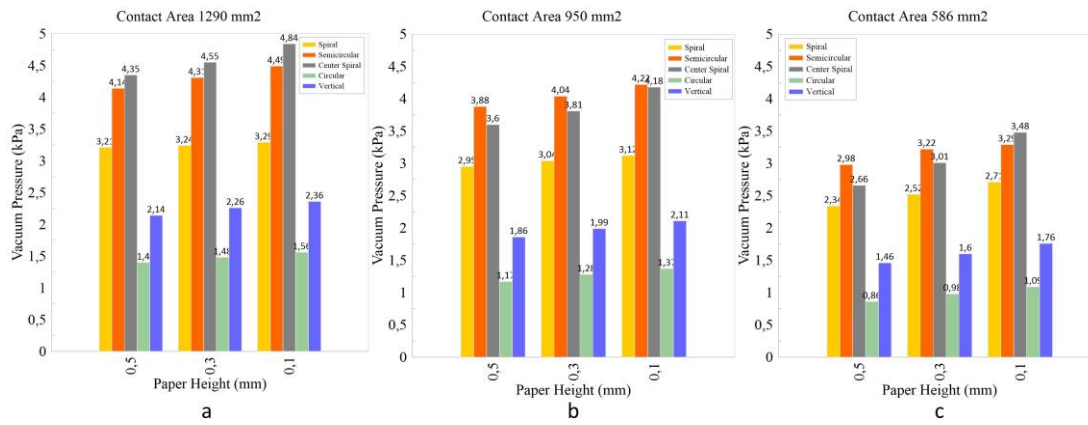


**Figure 6. 20 :** Paper Height and Vacuum Pressure, for Contact Areas: a) 586 mm<sup>2</sup>, b) 950 mm<sup>2</sup>, c) 1290 mm<sup>2</sup>.

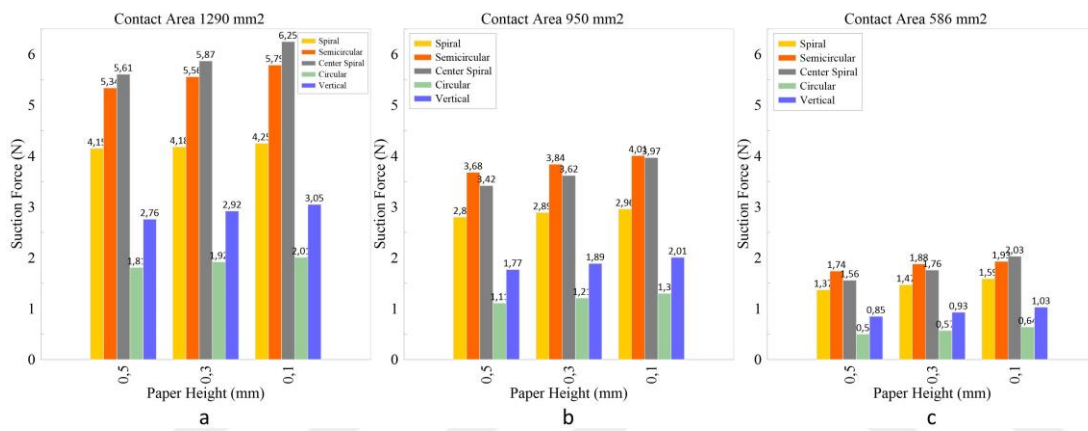


**Figure 6. 21 :** Paper Height and Suction Force, for Contact Areas a) 586 mm<sup>2</sup>, b) 950 mm<sup>2</sup>, c) 1290 mm<sup>2</sup>.

The maximum vacuum pressure and suction force obtained from the design cases are 4.84 kPa and 6.25 N with the parameter combination of 1290 mm<sup>2</sup> and 0.1 mm paper height for the center spiral design. In addition, it can be seen from the bar charts, decrease in paper heights resulted an increase in vacuum pressure and suction force in all design cases.

## 6.4 Discussion

In the scope of the study, positive pressure driven soft actuator design that is capable of creating vacuum and suction force is investigated. Rather than classical way of pumping the air out of the channels to create vacuum and suction force, it is proposed to use positive pressure in the air channels to deform the actuator into dome-like shape to achieve negative pressure in the vacuum cavity. In contrast to the literature given by Tang and Yin (2018) and Yang (2013), it is tried to create a comprehensive and

detailed finite element model to predict the vacuum and suction force performances of the proposed soft actuators. In addition to the finite element models, reference design (spiral design) is experimentally validated. Hence, it is found that numerical model is aligned with the result of experimental study.

Findings from the study shows that, it is possible to create vacuum and suction force with a positive pressure driven soft robotic actuator. Moreover, reference model design from the literature given by Tang and Yin (2018), which is spiral design, proved that it creates 7 N suction force (in normal direction) with 40-kPa air pressure, whereas in this study it is found with experimental study that the same air channel can provide 4.41 N with 13-kPa. In addition, numerical study results give the 4.25 N suction force capability with a parameter combination of contact area 1290-mm<sup>2</sup> and paper height level of 0.1 mm with 13-kPa air pressure in the cavity. It could be said that, based on the finding of this study, proposed actuator model (spiral design) is working with less air pressure than the actuator proposed by Tang and Yin (2018), hence it is capable of lifting 450 g mass. The disadvantage of the spiral design is found to be the unsymmetrical expansion from center to outer wall of the actuator. This characteristic design resulted in unequal wall thicknesses at the outer surface of the actuator and when the actuator is inflated displacement of the actuator was not equally distributed. On the other hand, the advantage of the spiral geometry is provided the central expansion to the actuator, hence it is found that typical expansion helps to create a dome-like shape. Possible improvement on the design could be done optimizing the wall thicknesses at the outermost wall, so when the actuator is inflated, it will be arranged that no extraordinary inflation will be at the outer surface of the actuator.

In contrasts to the spiral design geometry, a proposed unique air channel apart from the literature, which is called center spiral design, is showed the maximum vacuum pressure of 4.84 kPa and suction force of 6.25 N with the 13-kPa air pressure in the air channels. Hence, compared to the air channel designs proposed by Tang and Yin (2018) and Yang (2013), center spiral design is never put forward before this study. The advantage of the center spiral air channel compared to the spiral designed air channel is the equal wall thicknesses at the outermost surface of the actuator. In addition, air is distributed from center to the outer with help of discrete circles, this method is helped to diffuse equal and simultaneous airflow to the air channels as well

as it helps to create more dome like shape. Improvements of the center spiral design could be done validating the finite element model with experimental study.

Moreover, a detailed finite element model is set-up to predict different air channel geometries. Developed model is not only gives the deformation and stress results but also tracks the volume under the cavity, hence the fluid cavity sub-module is used to calculate pressure drop when the actuator starts vacuum. By this way, vacuum performance is tracked and suction force is calculated explicitly with theoretical calculations.

For the manufacturing stages, three mold is developed to produce same actuator body with different air channel geometries. Thus, the only required mold changes is restricted to air channels to produce faster and repeatable manufacturing of the actuators. Although the manufactured models are checked and overall performance approvable, 3D printed mold tolerances are not the tight enough to produce exact 3D models. Therefore, it might be useful to manufacture the actuators with metal molds. In addition, a vacuum chamber is required to prevent bubbles in the casted silicone, by this way it will be guaranteed that the liquid silicone will be homogenous when it is cured.

## 7. CONCLUSION

In this study, a bio-inspired pneumatic soft robotic actuator that creates a vacuum was examined with numerical and experimental methods. To prevent buckling of the soft and hyperelastic material of the actuator while creating a vacuum and suction force, positive pressure was used in the air channels rather than using direct vacuum techniques.

In total, five different actuator designs were proposed with the same outer geometry and different air channels. In addition, two main design parameters were selected namely the contact area and paper height (strain limiting layer) to investigate the vacuum and suction force performance regarding to three values of each parameter. In the design of the actuator, main body was inspired by octopus, which has the ability to create a vacuum with the help of its limbs. Besides, spiral design, which is one of the air channel designs, was selected as a reference model from the literature, and four unique air channel designs were derived to obtain more vacuum and suction force. Totally, nine design cases with combination of selected design parameters were investigated over five different actuators.

The spiral design of the actuator was selected to manufacture and testing. In order to manufacture the actuator, the gravity casting method was used by pouring the liquid silicone rubber into the 3D printed molds. Air pressure was applied with the help of an air pump (compressor) while a manometer was measured the channel pressure. Moreover, to test the suction force performance of the actuator, predetermined mass is lifted by actuator.

Finite element analysis results of the spiral design (reference model) was validated with the experimental results. Hence, due to the correlation between the results, same FEA model procedure was applied to the other actuator designs.

Based on the presented results, the center spiral and semicircular air channel designs were generated more vacuum and suction force than the other proposed designs with the percentage of 47 and 36 respectively.

This study was proved that positive pressure induced soft robotic actuators could be used in vacuum applications where safer human-robot interaction is necessary. Moreover, it presented the detailed FEA model of the soft pneumatic actuator that predicts the vacuum performance and suction force, which is validated with an experimental study. Further study requires a development of a framework and modular design that could be used to lift more weights, which consists of multiple center spiral actuators.



## 8. REFERENCES

- Abubakar, I. J., Myler, P., & Zhou, E.** (2016). Constitutive Modelling of Elastomeric Seal Material under Compressive Loading. *Modeling and Numerical Simulation of Material Science*, 06(02), 28–40. <https://doi.org/10.4236/mnsms.2016.62004>
- Agarwal, G., Besuchet, N., Audergon, B., & Paik, J.** (2016). Stretchable Materials for Robust Soft Actuators towards Assistive Wearable Devices. *Scientific Reports*, 6(September), 1–8. <https://doi.org/10.1038/srep34224>
- Bao, G., Fang, H., Chen, L., Wan, Y., Xu, F., Yang, Q., & Zhang, L.** (2018). Soft robotics: Academic insights and perspectives through bibliometric analysis. *Soft Robotics*, 5(3), 229–241. <https://doi.org/10.1089/soro.2017.0135>
- Bell, M. A., Pestovski, I., Scott, W., Kumar, K., Jawed, M. K., Paley, D. A., ... Wood, R. J.** (2018). Echinoderm-Inspired Tube Feet for Robust Robot Locomotion and Adhesion. *IEEE Robotics and Automation Letters*, 3(3), 2222–2228. <https://doi.org/10.1109/LRA.2018.2810949>
- Bhuse, P.** (2018). *Stress Analysis and Strength Evaluation of Scarf Adhesive Joint*. (February).
- Calisti, M., Corucci, F., Arienti, A., & Laschi, C.** (2015). Dynamics of underwater legged locomotion: Modeling and experiments on an octopus-inspired robot. *Bioinspiration and Biomimetics*, 10(4), 46012. <https://doi.org/10.1088/1748-3190/10/4/046012>
- Çivici, U. S., & Parlak, Z.** (2020). Soft Robot Motion under Surface Texture Effects. *Emerging Materials Research*, 9(1), 1–6. <https://doi.org/10.1680/jemmr.19.00072>
- Digumarti, K. M., Conn, A. T., & Rossiter, J.** (2017). Euglenoid-Inspired Giant Shape Change for Highly Deformable Soft Robots. *IEEE Robotics and Automation Letters*, 2(4), 2302–2307. <https://doi.org/10.1109/LRA.2017.2726113>
- Du Pasquier, C., Chen, T., Tibbits, S., & Shea, K.** (2019). Design and Computational Modeling of a 3D Printed Pneumatic Toolkit for Soft Robotics. *Soft Robotics*, 6(5), 657–663. <https://doi.org/10.1089/soro.2018.0095>
- Elsayed, Y., Vincensi, A., Lekakou, C., Geng, T., Saaj, C. M., Ranzani, T., ... Menciassi, A.** (2014). Finite Element Analysis and Design Optimization of a Pneumatically Actuating Silicone Module for Robotic Surgery Applications. *Soft Robotics*, 1(4), 255–262. <https://doi.org/10.1089/soro.2014.0016>
- Ge, D., Matsuno, T., Sun, Y., Ren, C., Tang, Y., & Ma, S.** (2015). Quantitative study on the attachment and detachment of a passive suction cup. *Vacuum*, 116, 13–20. <https://doi.org/10.1016/j.vacuum.2015.02.013>
- Hsu, Y. Y., Lucas, K., Davis, D., Elolampi, B., Ghaffari, R., Rafferty, C., &**

- Dowling, K.** (2013). Novel strain relief design for multilayer thin film stretchable interconnects. *IEEE Transactions on Electron Devices*, 60(7), 2338–2345. <https://doi.org/10.1109/TED.2013.2264217>
- Hu, W., Mutlu, R., Li, W., & Alici, G.** (2018). A structural optimisation method for a soft pneumatic actuator. *Robotics*, 7(2), 1–16. <https://doi.org/10.3390/robotics7020024>
- Iida, F., & Laschi, C.** (2011). Soft robotics: Challenges and perspectives. *Procedia Computer Science*, 7, 99–102. <https://doi.org/10.1016/j.procs.2011.12.030>
- Joo, S., & Baldwin, D. F.** (2010). Adhesion mechanisms of nanoparticle silver to substrate materials: Identification. *Nanotechnology*, 21(5). <https://doi.org/10.1088/0957-4484/21/5/055204>
- Laschi, C., & Cianchetti, M.** (2014). Soft robotics: New perspectives for robot bodyware and control. *Frontiers in Bioengineering and Biotechnology*, 2(JAN), 1–5. <https://doi.org/10.3389/fbioe.2014.00003>
- Laschi, C., Cianchetti, M., Mazzolai, B., Margheri, L., Follador, M., & Dario, P.** (2012). Soft robot arm inspired by the octopus. *Advanced Robotics*, 26(7), 709–727. <https://doi.org/10.1163/156855312X626343>
- Laschi, C., Mazzolai, B., & Cianchetti, M.** (2016). Soft robotics: Technologies and systems pushing the boundaries of robot abilities. *Science Robotics*, 1(1), 1–11. <https://doi.org/10.1126/scirobotics.aah3690>
- Lee, C., Kim, M., Kim, Y. J., Hong, N., Ryu, S., Kim, H. J., & Kim, S.** (2017). Soft robot review. *International Journal of Control, Automation and Systems*, 15(1), 3–15. <https://doi.org/10.1007/s12555-016-0462-3>
- Lin, H. T., Leisk, G. G., & Trimmer, B.** (2011). GoQBot: A caterpillar-inspired soft-bodied rolling robot. *Bioinspiration and Biomimetics*, 6(2). <https://doi.org/10.1088/1748-3182/6/2/026007>
- Majidi, C.** (2014). Soft Robotics: A Perspective - Current Trends and Prospects for the Future. *Soft Robotics*, 1(1), 5–11. <https://doi.org/10.1089/soro.2013.0001>
- Mosadegh, B., Polygerinos, P., Keplinger, C., Wennstedt, S., Shepherd, R. F., Gupta, U., ... Whitesides, G. M.** (2014). Pneumatic networks for soft robotics that actuate rapidly. *Advanced Functional Materials*, 24(15), 2163–2170. <https://doi.org/10.1002/adfm.201303288>
- Noritsugu, T., Takaiwa, M., & Sasaki, D.** (2008). Power assist wear driven with pneumatic rubber artificial muscles. *15th International Conference on Mechatronics and Machine Vision in Practice, M2VIP'08*, 539–544. <https://doi.org/10.1109/MMVIP.2008.4749589>
- Onal, C. D., & Rus, D.** (2012). A modular approach to soft robots. *Proceedings of the IEEE RAS and EMBS International Conference on Biomedical Robotics and Biomechatronics*, 1038–1045. <https://doi.org/10.1109/BioRob.2012.6290290>
- Qiao, S., Wang, L., Jeong, H., Rodin, G. J., & Lu, N.** (2017). Suction effects in cratered surfaces. *Journal of the Royal Society Interface*, 14(135). <https://doi.org/10.1098/rsif.2017.0377>
- Rafsanjani, A., Zhang, Y., Liu, B., Rubinstein, S. M., & Bertoldi, K.** (2018). Kirigami skins make a simple soft actuator crawl. *Science Robotics*, 3(15), 1–8.

<https://doi.org/10.1126/scirobotics.aar7555>

- Rogóż, M., Zeng, H., Xuan, C., Wiersma, D. S., & Wasylczyk, P.** (2016). Light-Driven Soft Robot Mimics Caterpillar Locomotion in Natural Scale. *Advanced Optical Materials*, 4(11), 1689–1694. <https://doi.org/10.1002/adom.201600503>
- Rus, D., & Tolley, M. T.** (2015). Design, fabrication and control of soft robots. *Nature*, 521(7553), 467–475. <https://doi.org/10.1038/nature14543>
- Sareh, S., Althoefer, K., Li, M., Noh, Y., Tramacere, F., Sareh, P., ... Kovac, M.** (2017). Anchoring like octopus: Biologically inspired soft artificial sucker. *Journal of the Royal Society Interface*, 14(135). <https://doi.org/10.1098/rsif.2017.0395>
- Schmitt, F., Piccin, O., Barbé, L., & Bayle, B.** (2018). Soft robots manufacturing: A review. *Frontiers Robotics AI*, 5(JUN). <https://doi.org/10.3389/frobt.2018.00084>
- Seok, S., Onal, C. D., Cho, K. J., Wood, R. J., Rus, D., & Kim, S.** (2013). Meshworm: A peristaltic soft robot with antagonistic nickel titanium coil actuators. *IEEE/ASME Transactions on Mechatronics*, 18(5), 1485–1497. <https://doi.org/10.1109/TMECH.2012.2204070>
- Shepherd, R. F., Ilievski, F., Choi, W., Morin, S. A., Stokes, A. A., Mazzeo, A. D., ... Whitesides, G. M.** (2011). Multigait soft robot. *Proceedings of the National Academy of Sciences of the United States of America*, 108(51), 20400–20403. <https://doi.org/10.1073/pnas.1116564108>
- Tang, Y., & Yin, J.** (2018). Design of Multifunctional Soft Doming Actuator for Soft Machines. *Advanced Materials Technologies*, 3(7), 1–8. <https://doi.org/10.1002/admt.201800069>
- Tang, Y., Zhang, Q., Lin, G., & Yin, J.** (2018). Switchable Adhesion Actuator for Amphibious Climbing Soft Robot. *Soft Robotics*, 5(5), 592–600. <https://doi.org/10.1089/soro.2017.0133>
- Taylor, T.** (2013). WebAL Comes of Age. *Artificial Life*, 19(3/4), 119–140. <https://doi.org/10.1162/ARTL>
- Trivedi, D., Rahn, C. D., Kier, W. M., & Walker, I. D.** (2008). Soft robotics: Biological inspiration, state of the art, and future research. *Applied Bionics and Biomechanics*, 5(3), 99–117. <https://doi.org/10.1080/11762320802557865>
- Wang, L., Ha, K. H., Qiao, S., & Lu, N.** (2019). Suction effects of crater arrays. *Extreme Mechanics Letters*, 30, 100496. <https://doi.org/10.1016/j.eml.2019.100496>
- Wang, Z., Polygerinos, P., Overvelde, J. T. B., Galloway, K. C., Bertoldi, K., & Walsh, C. J.** (2017). Interaction Forces of Soft Fiber Reinforced Bending Actuators. *IEEE/ASME Transactions on Mechatronics*, 22(2), 717–727. <https://doi.org/10.1109/TMECH.2016.2638468>
- Yang, S. X.** (2013). *Positive Pressure Induced Channeled Suction Cups*.
- Url-1** <<https://abaqus-docs.mit.edu/2017/English/SIMACAEANLRefMap/simaanl-c-surfacebasedcavityover.htm#hj-top>>, date retrieved 26.07.2020.
- Url-2** <<https://fea4eng.wordpress.com/2014/06/09/contact-problem-in-fea>>, date retrieved 30.07.2020.

**Url-3** <[http://web.mit.edu/calculix\\_v2.7/CalculiX/ccx\\_2.7/doc/ccx/node33.html](http://web.mit.edu/calculix_v2.7/CalculiX/ccx_2.7/doc/ccx/node33.html)>, date retrieved 31.07.2020.



## CURRICULUM VITAE



**Name Surname** : Umut Serdar ÇİVİCİ  
**Place and Date of Birth** : Sakarya/TURKEY - 1993  
**E-Mail** : civici17@itu.edu.tr, umut.civici@gmail.com

### EDUCATION :

- **B.Sc.** : 2017, Yıldız Technical University, Mechanical Engineering
- **B.Sc. (Erasmus)** : 2016, Otto-Von-Guericke University, Mechanical Engineering
- **M.Sc.** : 2020, Istanbul Technical University, Mechanical Engineering
- **M.Sc. (Erasmus)** : 2019, Delft University of Technology, Mechanical Engineering

### PROFESSIONAL EXPERIENCE:

- 2019-2020 FEV TURKEY, Mechanical Design Engineer.